IEEE Access
Multidisciplinary | Rapid Review | Open Access Journal

Received 15 September 2022, accepted 24 September 2022, date of publication 28 September 2022,
date of current version 7 October 2022.

Digital Object Identifier 10.1109/ACCESS.2022.3210687

RESEARCH ARTICLE

Estimation for Model Parameters and Maximum Power Points of Photovoltaic Modules Using Stochastic Fractal Search Algorithms

DUY C. HUYNH[1], (Senior Member, IEEE), MATTHEW W. DUNNIGAN[2], AND CORINA BARBALATA[3], (Member, IEEE)

[1]Electrical Engineering Department, HUTECH University, Ho Chi Minh City 70000, Vietnam
[2]Electrical Engineering Department, Heriot-Watt University, EH14 4AS Edinburgh, U.K.
[3]Mechanical and Industrial Engineering Department, Louisiana State University, Baton Rouge, LA 70803, USA

Corresponding author: Duy C. Huynh (hc.duy@hutech.edu.vn)

ABSTRACT The performance of a photovoltaic (PV) power generation system could be improved through the optimal control and operation of a PV module which is one of the fundamental components of this system. Thus, an appropriate PV module model along with precise knowledge of its parameters is necessary. This paper proposes a novel technique to estimate the source current, the saturation current of diodes, the shunt resistance, the series resistance, the ideality coefficient of diodes and the maximum power points (MPPs) of PV modules at the same time. This estimation problem can be described by the minimization of the root mean squared error (RMSE) of the powers obtained from the PV module through estimation and experiment. The improved stochastic fractal search (ISFS) algorithm is proposed to solve this minimization with two modifications. The first replaces the logarithmic function with the exponential function in the standard deviation of the diffusion technique to improve the exploration ability efficiently in the search space. The second utilizes the sine map instead of the uniform distribution in both the diffusion and update techniques for improving the performance of the ISFS algorithm. Numerical results demonstrate the remarkable ability of the ISFS algorithm in obtaining both the model parameters and MPPs of the PV module with high accuracy. The comparison shows that the ISFS algorithm outperforms other meta-heuristic algorithms such as a stochastic fractal search (SFS) algorithm, a particle swarm optimization (PSO) algorithm, and an improved particle swarm optimization (IPSO) algorithm in the proposed parameter estimation application.

INDEX TERMS Estimation, maximum power point, meta-heuristic algorithms, model parameter, photovoltaic modules.

I. INTRODUCTION

Solar energy, in general, and PV power systems, in particular, have become very popular for providing electrical energy for industrial production and domestic life. This is due to its numerous advantages such as infinite supply, simple extraction, quick installation, fewer emissions, less noise pollution, etc. [1]. The PV power systems have remarkably contributed to the power source structure of a power system and possess abundant potential. Problems related to how to exploit and operate efficiently the PV power system have been raised and addressed recently. The PV power system consists of PV modules which are interconnections of PV cells. Currently, a PV cell is popularly described by a single-diode model [2], [3]. This simple model shows an effective description of the PV cell. In some other applications, the PV cell needs to be modelled in more detail than the single-diode model, the PV cell is then described by a double-diode model [4]. As the detail of the PV cell is required to be increased in some situations, the PV cell is represented by a triple-diode model [5]. The utilization of the PV cell model should be analyzed and selected reasonably for each specific application to achieve the best descriptive effect. The specific application dictates which model is used. Amongst the above descriptions of the

The associate editor coordinating the review of this manuscript and approving it for publication was Qiang Li.

PV cell, the triple-diode model is the most complex model and the single-diode model is the simplest one. The single-diode model achieves the lowest computational complexity as well as the best trade-off between simplicity and precision. Thus, the single-diode model is chosen for the research described in this paper.

Table 1 show the definitions of the abbreviations utilized in this paper.

TABLE 1. Abbreviation.

Abbreviation	Definition
PV	Photovoltaic
MPP	Maximum power point
RMSE	Root mean squared error
SFS	Stochastic fractal search
ISFS	Improved stochastic fractal search
PSO	Particle swarm optimization
IPSO	Improved particle swarm optimization
GA	Genetic algorithm
ABC	Artificial bee colony
COA	Coyote optimization algorithm
FPA	Flower pollination algorithm
PSA	Projectile search algorithm
TGOA	Tree growth-based optimization algorithm
SOA	School-based optimization algorithm
GWO	Grey wolf optimization
SAIW	Simulated-annealing inertia weight
PO	Perturbation and observation
InC	Incremental conductance
STC	Standard testing condition
NOC	Normal operating condition
PID	Proportional-integral-derivative
PI	Proportional-integral
FL	Fuzzy logic
ANN	Artificial neural network

Additionally, Table 2 shows symbols which are utilized for mathematical descriptions of the estimation problem of model parameters and MPPs of PV modules.

Previous research works have shown that the electrical energy generated from the PV modules is significantly dependent on the operational conditions of the irradiance and the temperature [1]. Therefore, when these conditions are changed, the output power of the PV modules changes as well. This means that an appropriate control strategy should be proposed to ensure the adaptive and optimal operation of the PV modules. This is mainly modelled by the mathematical description of the PV module with elements of the current source, diodes, shunt resistance and series resistance of the PV cells. Then, the source current of the PV cell, saturation current and ideality coefficient of the diode and the shunt resistance and series resistance of the PV cell should be determined and updated during the operational process in the adaptive and optimal control problem of the PV module. However, manufacturers of the PV module only provide basic parameters such as voltage, U_{MPP}, current, I_{MPP}, and power, P_{MPP}, at an MPP; open-circuit voltage, U_{oc}; and short-circuit current, I_{sc}, in the STC with the irradiance, $G_{STC} = 1000$ (W/m^2), and the temperature, $T_{STC} = 298.15$ (^{0}K). This shows that the available specification of the PV modules in the datasheet of the manufacturer cannot fulfil the requirements of the adaptive and optimal control problem of the PV module.

TABLE 2. Nomenclature.

Symbol		Definition
$I^{SD}{}_c$ and $U^{SD}{}_c$	=	Load current (A) and voltage (V) of the PV cell
$I^{SD}{}_{ph}$	=	Source current of the PV cell (A)
$I^{SD}{}_D$ and $U^{SD}{}_D$	=	Current (A) and voltage (V) of the diode, D of the PV cell
$I^{SD}{}_0$	=	Saturation current of the diode, D of the PV cell (μA)
q	=	Charge on the electron, $q = 1.602 \times 10^{-19}$ (C)
k	=	Boltzmann constant, $k = 1.38 \times 10^{-23}$ (m^{2}kg/s^2)
$R^{SD}{}_{sh}$ and $R^{SD}{}_s$	=	Shunt and series resistances at the NOC of the PV cell (Ω)
$U^{SD}{}_t$	=	Temperature equivalent voltage of the PV cell (V)
a^{SD}	=	Ideality coefficient of the diode, D of the PV cell
N_{se} and N_{pa}	=	Numbers of PV cells in series and parallel in the PV module
U_{MPP}, I_{MPP}, and P_{MPP}	=	Voltage (V), current (A), and power (W) at an MPP of the PV module
$U_{oc,STC}$ and $I_{sc,STC}$	=	Open-circuit voltage (V) and short-circuit current (A) at STC of the PV module
U_{oc} and I_{sc}	=	Open-circuit voltage (V) and short-circuit current (A) at NOC of the PV module
I, U, and P	=	Load current (A), voltage (V), and power (W) of the PV module
I_{ph}	=	Source current of the PV module (A)
I_0	=	Saturation current of diodes of the PV module (μA)
$R_{sh,STC}$ and $R_{s,STC}$	=	Shunt and series resistances at STC of the PV module (Ω)
R_{sh} and R_s	=	Shunt and series resistances at NOC of the PV module (Ω)
U_t	=	Temperature equivalent voltage of the PV module (V)
a	=	Ideality coefficient of diodes of the PV module
G and G_{STC}	=	Solar irradiance at NOC and STC of the PV module, $G_{STC} = 1000$ (W/m^2)
T and T_{STC}	=	Temperature at NOC and STC of the PV module, $T_{STC} = 298.15$ (^{0}K)
μ_{Isc} and μ_{Uoc}	=	Temperature coefficients of the short-circuit current (A/^{0}C) and the open-circuit voltage (V/^{0}C) of the PV module
η	=	Constant, $\eta = 0.217$ [49]
N	=	Sample number
P_i^{est} and P_i^{exp}	=	The i^{th} power of the PV module obtained by the estimation and experiment (W)
$G(p_i, \delta)$	=	Gaussian function
δ	=	Standard deviation
R	=	Random number, $r \in [0,1]$
p_{best}	=	Best position of the particle
p_i	=	The i^{th} position of the particle, $i = 1, 2, ..., n_s$
n_s	=	Swarm size
n_G	=	Generation number
p'_i	=	New position of p_i
p_{r1} and p_{r2}:	=	Random positions of two particles in the first statistical technique
j	=	Index of the estimated parameters, $j = 1, 2, \ldots, d$
d	=	Number of the estimated parameters
γ_i	=	Selection probability of p_i
rank(p_i)	=	Fitness order of p_i, from best to worst
p'_{r1} and p'_{r2}	=	Random positions of the two particles in the second statistical technique
z_0	=	Initial point, $z_0 = 0.7$
z_i	=	The i^{th} point, $i = 0, 1, 2,...$
$z(i+1)$	=	The $(i+1)^{th}$ point

In addition, all parameters of the PV module always change under various operation conditions that are far from the STC. Therefore, it is important to obtain as complete a set of parameters of the PV module as possible for controlling adaptively and optimally the PV power system.

Recently, analytical techniques, numerical techniques, and meta-heuristic algorithm-based techniques have been introduced to achieve the model parameters of the PV module.

The analytical techniques are based on the relationship of the model parameters of the PV module between the STC and the various operating conditions as well as the data given by the manufacturers and experiments. It is realized that the algebraic equations of the PV module descriptions are non-linear expressions which must be simplified through an explicit model representation with first- and second-order approximation models [6], or Nyquist and Bode plots [7]. The above assumptions have reduced the accuracy of the estimated parameters. This parameter estimation problem is then solved by a truncated Taylor series-based solving technique [6], or Lambert function [8] showing the complexity of the analytical technique. Furthermore, initial estimations are also necessary in some cases [9]. If the initializations are not appropriate, this will affect the final convergence values of the parameter estimation problem and the error percentage of estimation will be significant.

Numerical techniques are presented to overcome several disadvantages of the analytical techniques. These include Newton-Raphson techniques [10], [11] and Levenberg-Marquardt techniques [12]. The disadvantages of the Newton-Raphson technique are the required computational burden, dependence on reasonably accurate initialization of estimated parameters, and poor convergence ability. The disadvantage of the Levenberg-Marquardt technique is the significant computational time since a Jacobian matrix is required as part of the parameter estimation procedure.

Recently, meta-heuristic algorithms have been applied to the parameter estimation of the PV module due to their reliability and efficiency. The meta-heuristic algorithms include GA, PSO, ABC, COA, FPA, PSA, TGOA, and SOA. The above algorithm-based estimation results show several disadvantages summarized in Table 3.

The above analyses show that the meta-heuristic algorithms have overcome many disadvantages of the previous parameter estimation techniques including the analytical and numerical techniques. However, these meta-heuristic algorithm-based techniques still have disadvantages such as being highly dependent on initializations, requiring many controlling parameters, and needing a large number of convergence iterations.

This paper proposes an ISFS algorithm-based parameter estimation technique for a PV module. The SFS algorithm is inspired by the random fractal growth phenomenon [21]. The SFS algorithm has fewer controlling parameters than other meta-heuristic algorithms [22], [23], [24]. In addition, the SFS algorithm has a high ability to achieve global optimal solutions with an acceptable number of iterations [21].

TABLE 3. Disadvantages of the previous parameter estimation studies.

Algorithm	Disadvantage	Reference
ABC algorithm	The exploitation ability is poor.	[2]
PSO-ABC algorithm	There are many tuning parameters.	[4]
COA	The procedure of producing new solution generations is complicated.	[5]
FPA	The algorithm performance mainly depends on a probability factor.	[11]
Binary-coded GA	• Solution of estimated parameters is affected by the restriction of string lengths; • There are many tuning parameters.	[13]
Real-coded GA	• The estimation procedure requires a longer estimation time; • There are many tuning parameters.	[14]
PSO algorithm	• The convergence process is premature; • There are many tuning parameters.	[15]
SIAW-PSO algorithm		[16]
Damping bound-handling approach-based PSO algorithm	There are many tuning parameters.	[17]
PSA		[18]
TGOA		[19]
SOA		[20]

These are the reasons why the SFS algorithm is popularly applied for solving various optimization problems.

TABLE 4. Applications of SFS algorithms.

SFS algorithm based-application	Reference
Parameter optimization for an auto-regressive exogenous model of twin rotor systems	[22]
Tracking state estimation of power systems	[23], [24]
Optimal design of Kalman filter	[25]
Frequency control application of an islanded microgrid	[26]
Economic dispatch application	[27]
Control application of DC motors	[28]
Control parameter optimization of conventional PID and FL-based PI controllers	[29], [30], [31]
Optimal path planning for UAVs	[32]
Optimization for the learning rate and the label smoothing regularization factor in a deep learning model of a convolutional neural network	[33]

Table 4 shows the wide applicability of the SFS algorithm in many various fields. The SFS algorithm-based achievements confirm the effectiveness and superiority of the SFS algorithm with its ability to maintain the balance between exploration and exploitation as well as the ease of being used in optimization applications with fewer tuning parameters. This means that the SFS algorithm is an appropriate choice to apply to the parameter estimation problem of the PV module. This is a novel proposal which has not been mentioned in

previous works. The ISFS algorithm is a variant of the SFS algorithm modifying the standard deviation of the diffusion technique and the uniform distribution of both the diffusion and updating techniques to improve the SFS algorithm performance. The ISFS algorithm is applied to estimate the model parameters of the PV module consisting of the source current of the PV module, I_{ph}; the saturation current, I_0 and ideality coefficient, a of the diode in the model of the PV module; and the shunt resistance, R_{sh} and series resistance, R_s of the PV module, which are unavailable in the datasheet of the manufacturers.

Additionally, the MPP of a PV module on the voltage-current (U-I) and voltage-power (U-P) characteristics should also be determined and updated to ensure that the PV module is always operated adaptively and optimally under various operational conditions. There are currently many techniques applied to determine MPPs of the PV modules such as PO algorithms [34], [35] and InC algorithms [36], [37]. Several previous studies show that the PO algorithm exhibits disadvantages such as oscillations around the MPP in steady-state conditions, deviations from the MPP in quickly changing conditions of the irradiance and temperature and requirements of an appropriate perturbation step size [38]. Similarly, the InC algorithm also has drawbacks such as slow convergence abilities with small perturbation step sizes, oscillations around the MPP in steady-state conditions with large perturbation step sizes and divergence of the operating point from the MPP [39]. To overcome the disadvantages of the PO algorithm, a step of determining the short-circuit current of the PV module is added during the search process of the MPP to ensure that there is no deviation from the MPP under quick variations of atmospheric conditions [34]. Additionally, the fixed perturbation step size is replaced by a variable one depending on power changes to ensure that the modified PO algorithm identifies the most accurate MPP during the search process [35]. Furthermore, the PO algorithm is also modified with the two-step-based technique. The first step is large for fast convergence to MPP as the power difference is large and the second step is small for eliminating oscillations around the MPP. The obtained results show that the modified PO algorithm is better than the traditional PO algorithm in the convergence performance as well as the accuracy of the achieved MPP of the PV module [40]. Additionally, the disadvantages of the InC algorithm are also overcome by combining the InC algorithm with the GWO algorithm-based PID controller to minimize steady-state oscillations at the MPP. The obtained results show the effectiveness of the improved InC algorithm with a reduction of steady-state oscillations around the MPP as well as better tracking performance of the MPP of the PV module [37]. In addition, the fixed step size in the InC algorithm is also improved by an adaptive step size with variations. This is based on how far away the current operating point is from a new MPP. The achievements of the modified InC algorithm show a feasible solution to improve the ability to determine MPPs with high accuracy and fast computational time [41]. It is realized that the above-presented improvements have not yet overcome all the disadvantages of the PO and InC algorithms. Each solution has been individual because the total solution can lead to complexity for the MPP tracking of the PV module. Another approach recommended for this problem is based on techniques such as the FL-based technique [42] and the ANN-based technique [43]. The FL-based technique is developed to identify the MPP of the PV module. This technique is based on FL rules which are set for each membership function. The results from using the FL-based technique are better than those obtained by the PO algorithm with the oscillations around the MPP in steady-state conditions being reduced [42]. By using the ANN-based technique, the voltage at the MPP is identified with the training data of the irradiance and temperature. The results of tracking MPPs of the PV module by using the ANN-based technique show superior tracking ability and speed compared to other techniques such as the PO algorithm-based technique and the InC algorithm-based technique. However, the ANN-based technique also has the disadvantage of requirements relating to training data and time. This affects the performance of the MPP tracking of the PV module [43]. Similarly, the above techniques of using ANN and FL still have disadvantages. Recently, the PSO algorithm-based technique was employed to identify MPPs of the PV module [44], [45]. The objective functions are formulated by the extracted power of the PV module. The PSO algorithm is applied to maximize the obtained power of the PV module under various atmospheric conditions. Importantly, this algorithm is also developed for the MPP tracking problem under partial shading conditions [46], [47]. However, the above analyses have shown the disadvantages of the PSO algorithm compared with the SFS and ISFS algorithms. Therefore, the ISFS algorithm is proposed to estimate the MPPs of the PV module under various irradiances and temperatures in this paper. The estimation of both the model parameters and MPPs of the PV module is novelly proposed in this paper which is necessary for improving the optimal exploitation efficiency of PV power systems. This combined estimation has been less mentioned in previous studies due to limitations of the analytical, numerical and meta-heuristic algorithm-based techniques [1], [2], [4] [25], [31]. Most of the previous studies have independently performed the estimation of the model parameters [2], [4] and MPPs [1], [25], [34] of the PV module. This inhibits the update of variations including the model parameters and MPPs of the PV module as synchronously and quickly as possible and certainly affects the results of the optimal and adaptive operation of the PV power system. The estimation results of the model parameters and MPPs of the PV modules using the ISFS algorithm are compared with the PSO, IPSO, and SFS algorithms to confirm the effectiveness of the proposal. The PSO algorithm is one of the popular meta-heuristic algorithms and is often selected to solve optimization problems because of its simplicity and ease of implementation. Comparisons in previous studies showed that the PSO algorithm is better than other meta-heuristic algorithms such as ABCs, FPAs, GAs, PSAs,

TGOAs, and SOAs in parameter estimation applications but there has not been yet any comparison between the PSO algorithm and the SFS algorithm, especially in the parameter estimation application of the PV module. Additionally, the objective of this paper is to solve the problem of estimating both model parameters and MPPs of the PV module simultaneously. Previous studies showed the disadvantages of using analytical techniques in the model parameter estimation application of the PV module. Moreover, it is very difficult to identify MPPs of the PV module by using analytical techniques. Most approaches for determining MPPs of the PV module have focused on PO and InC algorithms so far. The PO and InC algorithms are widely applied to identify MPPs of the PV module. However, it seems that these algorithms cannot be applied to estimate the model parameters of the PV module. The above analyses show that a proposal for the estimation of both the model parameters and MPPs of the PV module is a significant step forward. It is realized that the meta-heuristic algorithms are effective in this application. Amongst the meta-heuristic algorithms, the ISFS algorithm is proven to be superior to other meta-heuristic algorithms and is the best choice for this application. The above explanations show that the analytical technique-based parameter estimation approaches cannot be compared with the ISFS algorithm-based approaches as they cannot simultaneously estimate the model parameters and MPPs. This is the reason for not including the comparison between the SFS algorithms and analytical techniques. Instead, there should be only comparisons between the SFS algorithms and PSO algorithms.

The remainder of the paper is organized as follows. The model of a PV module is described in Section II. The estimation of the model parameters and MPPs of a PV module is presented in Section III. The experimental results achieved are presented in Section IV. Finally, the effectiveness of the proposed novel approach is highlighted in Section V.

II. MODELING OF A PV MODULE

A PV module is typically made up of interconnected PV cells. There are three popular models to describe a PV cell including the single-, double-, and triple-diode models. Amongst the models, the single-diode model achieves the lowest computational complexity as well as the best trade-off between simplicity and precision. Thus, the single-diode model is chosen to describe the PV cell in this paper. The description of the PV cell is shown in Fig. 1 [3].

Then, the mathematical model of the PV cell is given by:

$$I_c^{SD} = I_{ph}^{SD} - I_D^{SD} - \frac{U_D^{SD}}{R_{sh}^{SD}} \tag{1}$$

$$I_D^{SD} = I_0^{SD}\left[\exp\left(\frac{U_D^{SD}}{a^{SD}U_t^{SD}}\right) - 1\right] \tag{2}$$

$$U_D^{SD} = U_c^{SD} + R_s^{SD} I_c^{SD} \tag{3}$$

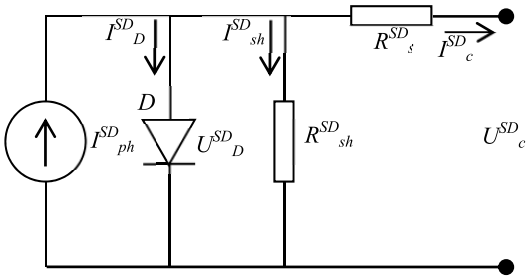

FIGURE 1. Modelling of a PV cell.

$$U_t^{SD} = \frac{kT}{q} \tag{4}$$

As a result, the load current of the PV cell is as follows:

$$I_c^{SD} = I_{ph}^{SD} - I_0^{SD}\left[\exp\left(\frac{q\left(U_c^{SD} + R_s^{SD} I_c^{SD}\right)}{a^{SD}kT}\right) - 1\right] - \frac{U_c^{SD} + R_s^{SD} I_c^{SD}}{R_{sh}^{SD}} \tag{5}$$

From the alignment of the PV cell, the PV module is described in Fig. 2 [48].

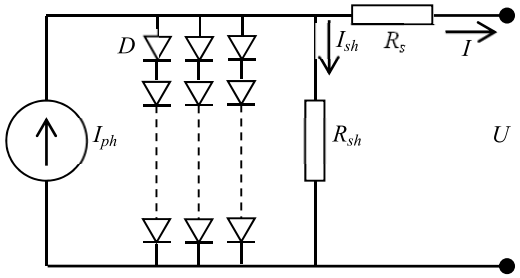

FIGURE 2. Modelling of a PV module.

The load current of the PV module is given by:

$$I = N_{pa} I_{ph} - N_{pa} I_0\left[\exp\left(\frac{q}{akT}\left(\frac{U}{N_{se}} + \frac{R_s I}{N_{pa}}\right)\right) - 1\right] - \frac{N_{pa}}{N_{se} R_{sh}} U + \frac{R_s}{R_{sh}} I \tag{6}$$

Then, the power of the PV module is as follows:

$$P = \frac{N_{pa} R_{sh} I_{ph} U}{(R_{sh} - R_s)} - \frac{N_{pa} R_{sh} I_0 U}{(R_{sh} - R_s)}\left[\exp\left(\frac{q}{akT}\left(\frac{U}{N_{se}} + \frac{R_s I}{N_{pa}}\right)\right) - 1\right] - \frac{N_{pa} U^2}{N_{se}\,(R_{sh} - R_s)} \tag{7}$$

$$P = f\left(I_{ph}, I_0, R_s, R_{sh}, a\right) \tag{8}$$

The irradiance and temperature effects on I_{ph}, I_0, R_{sh}, and R_s are given by [49] (9)–(13), as shown at the bottom of the next page.

III. ESTIMATION FOR MODEL PARAMETERS AND MPPs OF A PV MODULE BY USING SFS ALGORITHMS

A. ESTIMATION FOR MODEL PARAMETERS AND MPPs

It is realized that there are five model parameters, I_{ph}, I_0, R_s, R_{sh}, and a in (8) which need to be estimated from the model of the PV module. In addition, the MPPs also need to be identified, especially for the application of MPP tracking. The MPP, $P_{MPP}(U_{MPP}, I_{MPP})$ is unique in the U-I and U-P characteristics, Fig. 3.

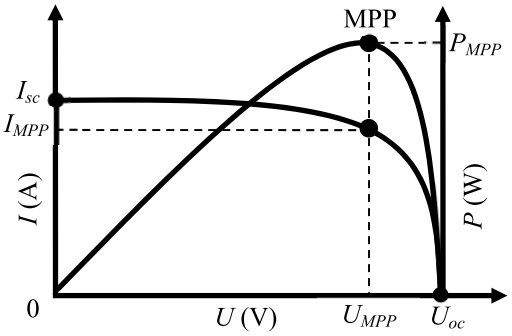

FIGURE 3. MPP description.

Therefore, the estimation problem is described by the minimization of the RMSE of the powers of the PV module between the estimation and experiment. Then, the model parameters, I_{ph}, I_0, R_s, R_{sh}, a and MPP, $P_{MPP}(U_{MPP}, I_{MPP})$ are estimated through the following RMSE minimization of the powers of the PV module.

In this paper, the RMSE of the powers of the PV module is the objective function given by:

$$RMSE = \sqrt{\frac{1}{N}\sum_{i=1}^{N}\left(P_i^{est} - P_i^{\exp}\right)^2} \tag{14}$$

The constraints of this parameter estimation problem are as follows:

$$I_{ph}^{\min} < I_{ph} < I_{ph}^{\max} \tag{15}$$

$$I_0^{\min} < I_0 < I_0^{\max} \tag{16}$$

$$R_s^{\min} < R_s < R_s^{\max} \tag{17}$$

$$R_{sh}^{\min} < R_{sh} < R_{sh}^{\max} \tag{18}$$

$$a^{\min} < a < a^{\max} \tag{19}$$

$$U_{MPP}^{\min} < U_{MPP} < U_{MPP}^{\max} \tag{20}$$

$$I_{MPP}^{\min} < I_{MPP} < I_{MPP}^{\max} \tag{21}$$

The SFS and ISFS algorithms are proposed to estimate the model parameters, I_{ph}, I_0, R_s, R_{sh}, a, and MPP, $P_{MPP}(U_{MPP}, I_{MPP})$ of the PV module respectively and are presented in more detail in the next sections.

B. ESTIMATION FOR MODEL PARAMETERS AND MPPs BY USING A SFS ALGORITHM

The SFS algorithm is based on the random fractal growth phenomenon in nature including the diffusion and update techniques in searching for solutions [21]. Each optimal position discovered by the SFS algorithm is an estimation result.

The Gaussian walk is utilized throughout the diffusion technique to produce points with a preset maximum diffusion number, n_{md}, encircling each particle for diffusing around its position and performing the exploitation.

The Gaussian walk is explained in detail below.

$$GW = G(p_i, \delta) + r \times (p_{best} - p_i) \tag{22}$$

The Gaussian function is described as follows:

$$G(p_i, \delta) = \frac{1}{\delta\sqrt{2\pi}} e^{-\frac{1}{2}\left(\frac{p_{best}-p_i}{\delta}\right)^2} \tag{23}$$

The standard deviation is given by:

$$\delta = \left|\frac{\log(n_G)}{n_G} \times (p_{best} - p_i)\right| \tag{24}$$

The position of each particle is updated in line with the positions of other particles throughout the updating technique. The exploration is then implemented by each particle using two statistical techniques.

$$I_{ph}(G,T) = \left(\frac{G}{G_{STC}}\right) I_{ph}(T) \tag{9}$$

$$I_{ph}(T) = I_0(T)\exp\left[\frac{V_{oc,STC} + \mu_{U_{oc}}(T - T_{STC})}{aN_{se}U_t(T)}\right] + \frac{\left(V_{oc,STC} + \mu_{U_{oc}}(T - T_{STC})\right)}{R_{sh}} \tag{10}$$

$$I_0(G,T) = \frac{\left[\begin{array}{l}(1 + R_s/R_{sh})\left(I_{sc,STC} + \mu_{I_{sc}}(T - T_{STC})\right) \\ -\left(U_{oc,STC} + \mu_{U_{oc}}(T - T_{STC}) + aN_{se}U_t \ln(G)\right)/R_{sh}\end{array}\right]}{\left[\begin{array}{l}\exp\left(\frac{(U_{oc,STC} + \mu_{U_{oc}}(T - T_{STC}) + aN_{se}U_t \ln(G))}{aN_{se}U_t}\right) \\ -\exp\left(\frac{(I_{sc,STC} + \mu_{I_{sc}}(T - T_{STC}))R_s}{aN_{se}U_t}\right)\end{array}\right]} \tag{11}$$

$$R_{sh}(G) = \left(\frac{G_{STC}}{G}\right) R_{sh,STC} \tag{12}$$

$$R_s(G,T) = \frac{T}{T_{STC}}\left(1 - \eta \ln\frac{G}{G_{STC}}\right) R_{s,STC} \tag{13}$$

The first statistical technique is described by:

$$p_i'(j) = \begin{cases} p_{r1}(j) - r \times [p_{r2}(j) - p_i(j)] & if\ \gamma_i < r \\ p_i(j) & otherwise \end{cases} \quad (25)$$

$$\gamma_i = 1 - \frac{rank(p_i)}{n_s} \quad (26)$$

The second statistical technique is described by:

$$p_i'(j) = \begin{cases} p_i(j) - r \times \left[p_{r1}'(j) - p_{best}(j)\right] & if\ r < 0.5 \\ p_i(j) + r \times \left[p_{r1}'(j) - p_{r2}'(j)\right] & otherwise \end{cases} \quad (27)$$

It is realized that the SFS algorithm performance can be improved through the initialization of the solutions, the creation of a new solution and the update of the solution. This results in the reduction of the computational time and increased accuracy of the estimation of the model parameters, I_{ph}, I_0, R_s, R_{sh}, a, and MPP, $P_{MPP}(U_{MPP}, I_{MPP})$ of the PV module. This paper proposes an improved SFS algorithm with mentioned modifications. The detail of the ISFS algorithm is presented in the next section.

C. ESTIMATION FOR MODEL PARAMETERS AND MPPs BY USING A ISFS ALGORITHM

As mentioned, the ISFS algorithm modifies the procedures of the initialization of the solutions, the creation of a new solution, and the update of the solution in the SFS algorithm.

It is realized that the essential execution of the meta-heuristic algorithms, in general, and the SFS, in particular, is more typically the randomization of each particle using a uniform distribution as well as dealing with challenges of non-linear and multi-modal complicated objective functions. Chaotic maps are then recommended to utilize as an alternative to a random uniform distribution [50], [51], [52]. Amongst the chaotic maps, a sine map is one of the simplest and most easily applied chaotic maps chosen to improve the performance of the SFS algorithm in this paper [53], [54]. The random uniform distribution is represented by the sine map in the initialization of the solutions. This creates a diverse initial solution space that contributes to improving the exploitation ability of the algorithm.

The sine map is shown as follows:

$$z_{(i+1)} = \sin(\pi z_i) \quad (28)$$

Additionally, previous studies have shown that the exploration and exploitation ability of the meta-heuristic algorithms are extremely important [50], [51], [52]. This certainly applies to the SFS algorithm as well. Therefore, in the creation of a new solution for the ISFS algorithm, the standard deviation in the diffusion technique is computed via the exponential function instead of the logarithmic function for enhancing the exploration ability of the algorithm [55]. This modification allows limiting the number of Gaussian jumps as the number of iterations increments. Then, the exploration performance of the ISFS algorithm is improved in the search space.

The standard deviation is re-written as:

$$\delta = \left| \frac{\exp(-n_G)}{n_G} \times (p_{best} - p_i) \right| \quad (29)$$

Moreover, the Gaussian walk is also modified with the sine map and re-described for improving the quality of the solutions as follows:

$$GW = G(p_i, \delta) + z \times (p_{best} - p_i) \quad (30)$$

Simultaneously, the first and second updating techniques are respectively modified with the sine map as follows:

$$p_i'(j) = \begin{cases} p_{r1}(j) - z \times [p_{r2}(j) - p_i(j)] & if\ \gamma_i < z \\ p_i(j) & otherwise \end{cases} \quad (31)$$

$$p_i'(j) = \begin{cases} p_i(j) - z \times \left[p_{r1}'(j) - p_{best}(j)\right] & if z < 0.5 \\ p_i(j) + z \times \left[p_{r1}'(j) - p_{r2}'(j)\right] & otherwise \end{cases} \quad (32)$$

The ISFS algorithm-based estimation results are compared with the SFS estimation results. This comparison validates the effectiveness of the proposed ISFS algorithm in the estimation application of the model parameters, $I_{ph}, I_0, R_s, R_{sh}, a$, and MPP, $P_{MPP}(U_{MPP}, I_{MPP})$ of the PV module. In addition, the ISFS algorithm-based estimation results are compared with the estimation results achieved by the PSO and IPSO algorithms to re-confirm the effectiveness and superiority of the ISFS algorithm in the estimation application of the model parameters, I_{ph}, I_0, R_s, R_{sh}, a, and MPP, $P_{MPP}(U_{MPP}, I_{MPP})$, of the PV module for adaptive and optimal control problems.

In this SFS and ISFS algorithm-based parameter estimation application of the PV module, each position of the particle is described by an estimation vector, $\boldsymbol{p}$, as follows:

$$p = [I_{ph}, I_0, R_s, R_{sh}, a, U_{MPP}, I_{MPP}] \quad (33)$$

There are seven parameters of the PV module that require to be estimated in this paper. These are the basic and necessary parameters required in the control and operation problems of the PV module.

Fig. 4 is the flowchart of the SFS algorithms. In this flowchart, the SFS algorithm is shown with the function blocks with solid and black lines on the left-hand side whereas the ISFS algorithm is shown with dashed and blue lines on the right-hand side. In the ISFS algorithm, the solution initialization, the procedure of creating a new solution, and the procedure of updating the solution are modified to improve the performance of the SFS algorithm. The solution initialization of the ISFS algorithm is modified and based on the sine map which creates variety in the search space of the solutions. This improves the exploitation ability of the ISFS algorithm. Moreover, the procedures of creating a new solution and updating the solution are also based on the sine map which enhances the exploration ability of the ISFS algorithm. Thus, the algorithm performance of the ISFS algorithm is improved in terms of the convergence value and speed. This results in the improvement of the estimation results of the model parameters and MPPs of the PV module.

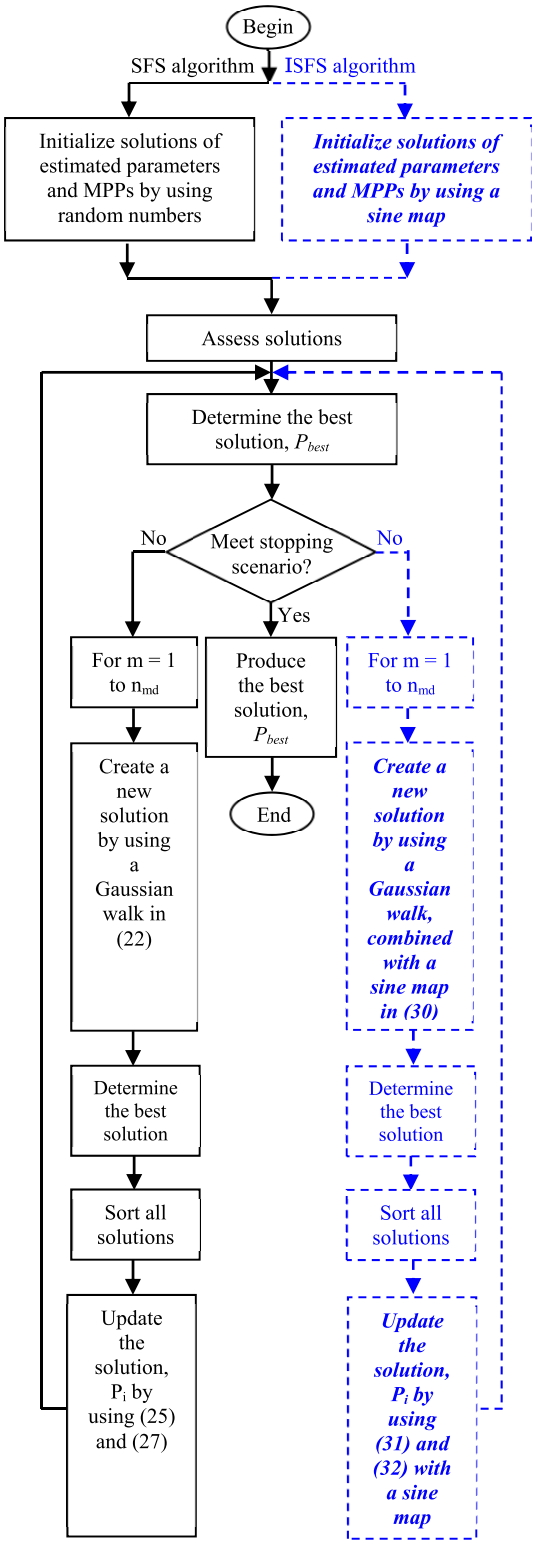

FIGURE 4. Flowchart of SFS algorithms.

The experiments and the ISFS, SFS, IPSO, and PSO algorithm-based estimations of the model parameters and MPPs of the PV module are described in the next section.

This is to confirm the effectiveness of the proposal in the estimation application of the PV module.

D. PARAMETER TUNING OF META-HEURISTIC ALGORITHMS

The SFS, ISFS, PSO and IPSO algorithms are the meta-heuristic algorithms proposed to be used for the parameter estimation application of the PV module in this paper. In the meta-heuristic algorithm-based applications, the selection of optimal parameters of the meta-heuristic algorithms is a great challenge affecting the quality of achieved optimal solutions [56]. There are two kinds of parameter settings of the meta-heuristic algorithms including parameter tuning, known as off-line tuning; and parameter control, known as on-line tuning [57]. In this paper, parameter tuning is described and applied to determine optimal parameters of the SFS, ISFS, PSO, and IPSO algorithms because of the appropriateness and requirement of the parameter estimation application of the PV module. The parameter tuning allows identifying the optimal parameters of the SFS, ISFS, PSO and IPSO algorithms before the given algorithms are applied to estimate the parameters of the PV module. The values of algorithm parameters are fixed in the initialization and do not vary during the operation.

It is realized that the problem of determining the optimal tuning parameters of the SFS, ISFS, PSO and IPSO algorithms can be formulated as optimization problems. All these algorithms are optimization algorithms. Therefore, the optimization of the meta-heuristic parameters is called meta-optimization. Additionally, this paper proposes to solve the meta-optimization by applying meta-heuristic algorithms. Then, it is called the meta-meta-heuristic approach consisting of the meta-level and the base level [58], [59].

A meta-heuristic solves the meta-optimization based on populations of solutions at the meta-level. A solution is a set of the parameters of the meta-heuristic. The values of the swarm size, maximum iteration and maximum diffusion are optimized in the SFS and ISFS algorithms whereas the values of the swarm size, maximum iteration, individual cognition coefficient, social learning coefficient and inertia weight are optimized in the PSO and IPSO algorithms.

Each solution of the meta-level corresponds to an independent meta-heuristic at the base level working on populations of solutions of the original optimization problem in general and the parameter estimation problem of the PV module in particular.

IV. EXPERIMENTAL RESULTS

The commercial multi-crystal PV module, Kyocera KC200GT-215, is used to conduct the experiments in the estimation problem of the model parameters and MPPs. Table 5 is the parameters in the datasheet of the commercial multi-crystal PV module, Kyocera KC200GT-215, which cannot fully satisfy the parameter requirements in the control and operation issues of the PV module. In addition, the values of the parameters in the datasheet are obtained in the STC with the irradiance, $G_{STC} = 1000$ (W/m^2), and temperature, $T_{STC} = 298.15$ (^{0}K). When the irradiance, G,

TABLE 5. Parameters in the datasheet of the commercial multi-crystal PV module, Kyocera KC200GT-215.

Parameter	Value
Power at the MPP, P_{MPP}(W)	200
Voltage at the MPP, V_{MPP}(V)	26.3
Current at the MPP, I_{MPP}(A)	7.61
Open-circuit voltage, V_{oc}(V)	32.9
Short-circuit current, I_{sc}(A)	8.21
Temperature coefficient of I_{sc}, μ_{Isc}(A/^{0}C)	-1.23×10^{-1}
Temperature coefficient of V_{oc}, μ_{Voc}(A/^{0}C)	3.18×10^{-3}
Number of PV cells in series, N_{se}	54
Number of PV cells in parallel, N_{pa}	1

and temperature, T, are changed and are different from the irradiance, G_{STC}, and temperature, T_{STC}, in the STC, the parameters in the datasheet will change accordingly. This re-confirms that the estimation of the model parameters and MPPs of the PV module is necessary to satisfy the requirements of obtaining additional parameters which are unavailable in the datasheet of the manufacturers as well as to update the variations of the model parameters and MPPs during the control and operation process of the PV module. The sample number of the power of the PV module, Kyocera KC200GT-215, N, is 34.

TABLE 6. Parameters of the SFS and ISFS algorithms.

Parameter and procedure	Value	
	SFS algorithm	ISFS algorithm
Swarm size, n_s	50	50
Maximum iteration, $Iter_{max}$	1000	1000
Maximum diffusion, n_{md}	1	1
Procedure of initializing solutions	Random distribution	Sine map by using (29)
Procedure of creating a new solution	Gaussian walk by using (22)	Sine map-based Gaussian walk by using (30)
Procedure of updating the solution	Update by using (25) and (27)	Sine map-based update by using (31) and (32)

TABLE 7. Parameters of The PSO and IPSO Algorithms.

Parameter	Value	
	PSO algorithm	IPSO algorithm
Swarm size, n_s	50	50
Maximum iteration, $Iter_{max}$	1000	1000
Individual cognition coefficient, c_1	2	2
Social learning coefficient, c_2	2	2
Inertia weight, w	0.6	Sine map

Tables 6-7 show the parameters of the SFS, ISFS, PSO and IPSO algorithms. Table 6 are the parameters of the SFS and ISFS algorithms where the swarm size, n_s, is 50; the maximum iteration number, $Iter_{max}$, is 1000; the maximum diffusion number, n_{md}, is 1. These parameters are achieved by using the meta-meta-heuristic approach.

Furthermore, Table 6 also shows the difference between the SFS and ISFS algorithms in the solution initialization, the procedure of creating a new solution and the procedure of updating the solution. These chaotic map-based modifications are to create variety in the search space of the solutions for enhancing the exploitation and exploration abilities of the ISFS algorithm through the procedures of creating a new solution and updating the solution. These are expected to improve the ISFS algorithm performance through convergence value and speed. The sine map is the chaotic map chosen and is applied in the procedures for initializing solutions, creating a new solution and updating the solution in the ISFS algorithm.

To compare and validate the effectiveness of the proposal using the ISFS algorithm-based estimation application, the PSO and IPSO algorithms are introduced and applied to estimate the model parameters and MPPs of the PV module [60]. The comparisons between the ISFS, SFS, PSO and IPSO are implemented with the same condition of the swarm size, n_s, and the maximum iteration number, $Iter_{max}$. Similarly, by using the meta-meta-heuristic, the parameters of the PSO and IPSO algorithms are shown in Table 7, where the swarm size, n_s, is 50; the maximum iteration number, $Iter_{max}$, is 1000; the individual cognition and social learning coefficients, c_1 and c_2, are both 2 respectively; the inertia weights, w, are 0.6 and the sine map in the PSO and IPSO algorithms respectively. These parameters are achieved by using the meta-meta-heuristic approach. The difference between the PSO and IPSO algorithms is in the inertia weight [61], [62]. The chaotic inertia weight creates the best balance between local and global search processes. This improves the convergence performance of the PSO algorithm.

TABLE 8. Estimation space of the model parameters and MPPs of the PV module.

Parameter	Limit	
	Min	Max
Source current of the PV module, I_{ph}(A)	0	10
Saturation current of diodes of the PV module, I_0(μA)	0	1
Series resistance of the PV module, R_s(Ω)	0	2
Shunt resistance of the PV module, R_{sh}(Ω)	0	10000
Ideality coefficient of diodes of the PV module, a	1	2
Voltage of the PV module at the MPP, U_{MPP}(V)	0	50
Current of the PV module at the MPP, I_{MPP}(A)	0	10

Table 8 is the estimation space of the model parameters, I_{ph}, I_0, R_s, R_{sh}, a, and MPP, $P_{MPP}(U_{MPP}, I_{MPP})$, of the PV module showing the minimum and maximum limitations of each estimated parameter.

TABLE 9. Scenario of various irradiance and temperature conditions.

Scenario	Irradiance, G(W/m^2)	Temperature, T(^{0}K)
1	1000	298.15
2	800	298.15
3	600	298.15
4	400	298.15
5	200	298.15
6	1000	323.15
7	1000	348.15

TABLE 10. Estimation results of the model parameters and MPPs of The PV module by using The PSO, IPSO, SFS, and ISFS algorithms with G = 200-1000 (W/m^2) and T = 298.15-348.15 (^{0}K).

Sce-na-rio	Para-meter	Algorithm			
		PSO	IPSO	SFS	ISFS
1	I_{ph}(A)	7.2811	7.6289	7.7501	8.2010
	I_0(μA)	0.1573	0.1666	0.1682	0.1781
	R_s(Ω)	0.1950	0.2057	0.2079	0.2201
	R_{sh}(Ω)	846.7000	886.2949	895.5639	951.9300
	a	1.1801	1.2416	1.2554	1.3340
	U_{MPP}(V)	24.0014	25.1628	25.5010	27.0460
	I_{MPP}(A)	6.7010	7.0455	7.1196	7.5699
	P_{MPP}(W)	160.8334	177.2845	181.5569	204.7355
2	I_{ph}(A)	5.8110	6.1182	6.1968	6.5680
	I_0(μA)	0.1225	0.1301	0.1305	0.1388
	R_s(Ω)	0.2380	0.2516	0.2535	0.2688
	R_{sh}(Ω)	1031.1468	1088.0250	1101.2200	1169.5500
	a	1.1680	1.2280	1.2406	1.3170
	U_{MPP}(V)	23.0430	24.3072	24.4976	26.0292
	I_{MPP}(A)	5.5086	5.7925	5.8456	6.2176
	P_{MPP}(W)	126.9347	140.7995	143.2032	161.8392
3	I_{ph}(A)	4.3545	4.5963	4.6474	4.9390
	I_0(μA)	0.0915	0.0967	0.0975	0.1035
	R_s(Ω)	0.3090	0.3245	0.3277	0.3478
	R_{sh}(Ω)	1369.8412	1438.6591	1460.8400	1545.8700
	a	1.1570	1.2174	1.2341	1.3080
	U_{MPP}(V)	22.2501	23.3711	23.6405	25.0227
	I_{MPP}(A)	4.2070	4.4089	4.4609	4.7300
	P_{MPP}(W)	93.6062	103.0408	105.4579	118.3574
4	I_{ph}(A)	2.9070	3.0710	3.1003	3.2850
	I_0(μA)	0.0610	0.0644	0.0651	0.0692
	R_s(Ω)	0.4590	0.4826	0.4892	0.5179
	R_{sh}(Ω)	2006.1324	2115.4294	2138.5300	2273.5800
	a	1.1260	1.1976	1.2066	1.2770
	U_{MPP}(V)	21.2175	22.4192	22.6751	23.9991
	I_{MPP}(A)	2.7920	2.9522	2.9684	3.1422
	P_{MPP}(W)	59.2393	66.1860	67.3088	75.4100
5	I_{ph}(A)	1.4105	1.4906	1.5034	1.5920
	I_0(μA)	0.0310	0.0375	0.0332	0.0352
	R_s(Ω)	0.8905	0.9353	0.9462	1.0014
	R_{sh}(Ω)	3904.5791	4085.1048	4145.9200	4389.3600
	a	1.0950	1.1556	1.1706	1.2390
	U_{MPP}(V)	20.2505	21.2179	21.5420	22.8106
	I_{MPP}(A)	1.3750	1.4487	1.4705	1.5568
	P_{MPP}(W)	27.8444	30.7384	31.6775	35.5115
6	I_{ph}(A)	7.3190	7.7098	7.8312	8.2880
	I_0(μA)	0.1826	0.1915	0.1951	0.2058
	R_s(Ω)	0.2711	0.2882	0.2905	0.3077
	R_{sh}(Ω)	843.1143	889.6346	896.9100	952.1200
	a	1.2142	1.2711	1.2872	1.3648
	U_{MPP}(V)	21.3611	22.5320	22.7078	24.0400
	I_{MPP}(A)	6.6070	6.9901	7.0806	7.4969
	P_{MPP}(W)	141.1328	157.5009	160.7848	180.2255
7	I_{ph}(A)	7.4390	7.8006	7.9063	8.3770
	I_0(μA)	0.1911	0.2026	0.2052	0.2176
	R_s(Ω)	0.3810	0.4016	0.4061	0.4308
	R_{sh}(Ω)	844.1211	890.0750	898.2300	953.7500
	a	1.2295	1.2974	1.3105	1.3921
	U_{MPP}(V)	18.5700	19.6566	19.8010	20.9641
	I_{MPP}(A)	6.5080	6.8275	6.9073	7.3199
	P_{MPP}(W)	120.8536	134.2054	136.7714	153.4551

Table 9 shows the scenarios of various irradiance and temperature conditions with G = 200-1000 (W/m^2) and T = 298.15-348.15 (^{0}K) considered in the estimation problem of the model parameters and MPPs of the PV module.

Table 10 is the estimation results of the model parameters and MPPs of the PV module by using the PSO, IPSO, SFS, and ISFS algorithms with the irradiance, G = 200-1000 (W/m^2) and the temperature, T = 298.15-348.15 (^{0}K).

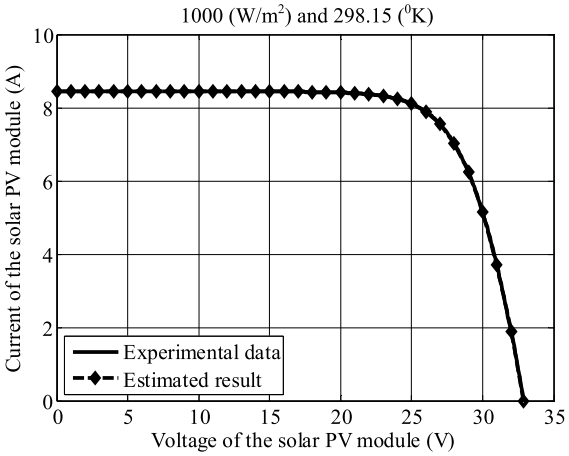

FIGURE 5. $U-I$ **characteristics of the PV module obtained by experiment and ISFS algorithm-based estimation with G = 1000 (W/m^2) and T = 298.15 (^{0}K).**

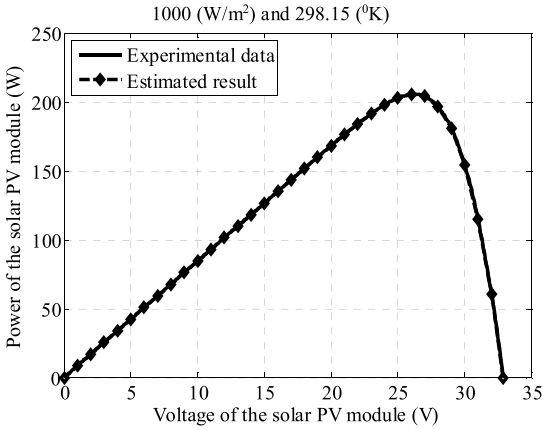

FIGURE 6. $U-P$ **characteristics of the PV module obtained by experiment and ISFS algorithm-based estimation with G = 1000 (W/m^2) and T = 298.15 (^{0}K).**

Figs. 5-6 show the U-I and U-P characteristics of the PV module obtained by the experiment and ISFS algorithm-based estimation with G = 1000 (W/m^2) and T = 298.15 (^{0}K). These characteristics confirm the estimation accuracy of the model parameters, I_{ph} = 8.2010 (A), I_0 = 0.1781 (μA), R_s = 0.2201 (Ω), R_{sh} = 951.9300 (Ω), a = 1.3340; and the MPP, U_{MPP} = 27.0460 (V), I_{MPP} = 7.5699 (A), P_{MPP} = 204.7355 (W) of the PV module by using the ISFS algorithm.

In another scenario with G = 800 (W/m^2) and T = 298.15 (^{0}K), Table 9, the U-I and U-P characteristics of the PV module obtained by the experiment and ISFS algorithm-based estimation are shown in Figs. 7-8. These characteristics confirm the estimation accuracy of the model parameters, I_{ph} = 6.5680 (A), I_0 = 0.1388 (μA), R_s = 0.2688 (Ω), R_{sh} = 1169.5500 (Ω), a = 1.3170; and the MPP, U_{MPP} = 26.0292 (V), I_{MPP} = 6.2176 (A), P_{MPP} = 161.8392 (W) of the PV module when using the ISFS algorithm.

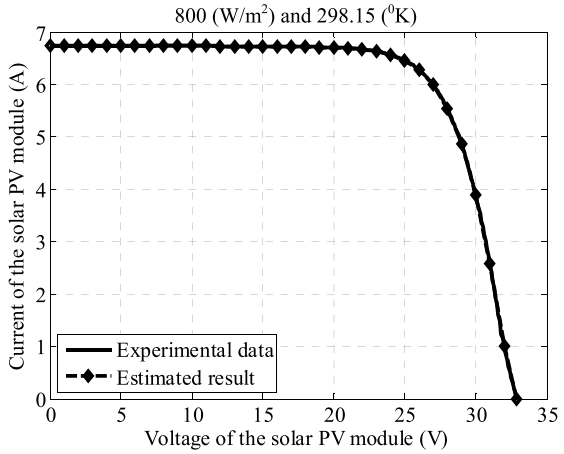

FIGURE 7. $U-I$ characteristics of the PV module obtained by experiment and ISFS algorithm-based estimation with $G = 800$ (W/m^2) and $T = 298.15$ (^{0}K).

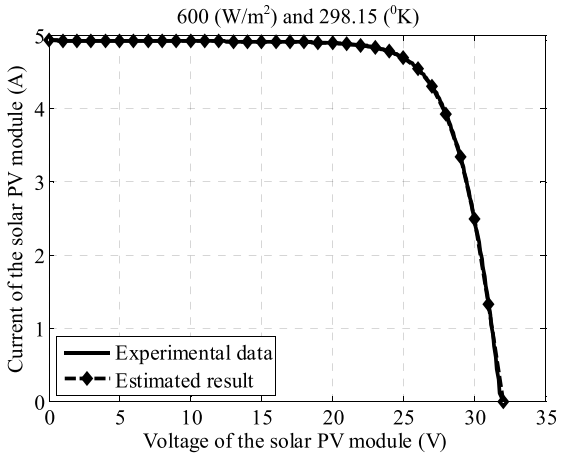

FIGURE 9. $U-I$ characteristics of the PV module obtained by experiment and ISFS algorithm-based estimation with $G = 600$ (W/m^2) and $T = 298.15$ (^{0}K).

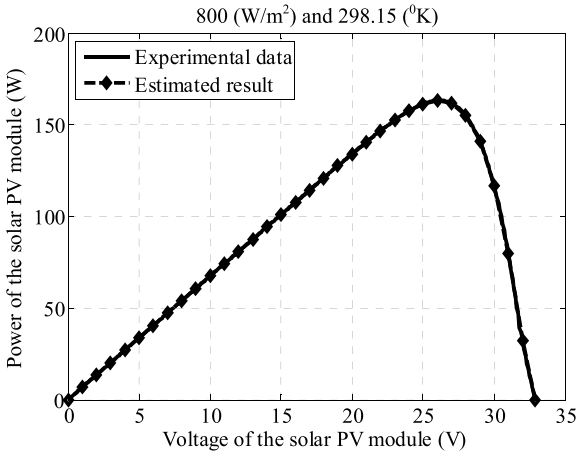

FIGURE 8. $U-P$ characteristics of the PV module obtained by experiment and ISFS algorithm-based estimation with $G = 800$ (W/m^2) and $T = 298.15$ (^{0}K).

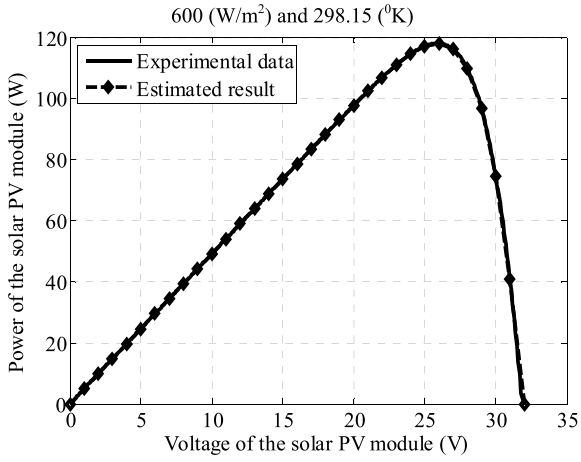

FIGURE 10. $U-P$ characteristics of the PV module obtained by experiment and ISFS algorithm-based estimation with $G = 600$ (W/m^2) and $T = 298.15$ (^{0}K).

If scenario 2 is compared with scenario 1, then it is realized that G = 1000-800 (W/m^2) is decreased and $T = 298.15$ (^{0}K) is constant. This leads to the model parameters, I_{ph}, I_0, and a decreasing and the other model parameters, R_{sh} and R_s increasing with the power at the MPP, P_{MPP}, being reduced.

In scenario 3, the U-I and U-P characteristics of the PV module obtained experimentally are compared to the ISFS algorithm-based estimation shown in Figs. 9-10. These characteristics show that the ISFS algorithm-based estimation results of the model parameters, $I_{ph} = 4.9390$ (A), $I_0 = 0.1035$ (μA), $R_s = 0.3478$ (Ω), $R_{sh} = 1545.8700$ (Ω), $a = 1.3080$; and the MPP, $U_{MPP} = 25.0227$ (V), $I_{MPP} = 4.7300$ (A), $P_{MPP} = 118.3574$ (W) of the PV module are accurate.

Scenario 3 is compared with scenarios 1 and 2. The comparison shows that G = 1000-600 (W/m^2) is decreased and $T = 298.15$ (^{0}K) is constant, the model parameters, I_{ph}, I_0, and a decrease and the other model parameters, R_{sh} and R_s, increase with the power at the MPP, P_{MPP}, being reduced.

The U-I and U-P characteristics for scenario 4, Figs. 11-12, validate the accuracy of the ISFS algorithm-based estimation results of the model parameters, $I_{ph} = 3.2850$ (A), $I_0 = 0.0692$ (μA), $R_s = 0.5179$ (Ω), $R_{sh} = 2273.5800$ (Ω), $a = 1.2770$; and the MPP, $U_{MPP} = 23.9991$ (V), $I_{MPP} = 3.1422$ (A), $P_{MPP} = 75.4100$ (W). Scenario 4 is next compared with scenarios 1-3. The comparison shows that $G = 1000$-400 (W/m^2) is decreased and $T = 298.15$ (^{0}K) is constant. The model parameters, I_{ph}, I_0, and a decrease, the other model parameters, R_{sh} and R_s, increase with the power at the MPP, P_{MPP}, being reduced.

Similarly, the accuracy of the ISFS algorithm-based estimation results of the model parameters, $I_{ph} = 1.5920$ (A), $I_0 = 0.0352$ (μA), $R_s = 1.0014$ (Ω), $R_{sh} = 4389.3600$ (Ω), $a = 1.2390$; and the MPP, $U_{MPP} = 22.8106$ (V), $I_{MPP} = 1.5568$ (A), $P_{MPP} = 35.5115$ (W) of the PV module is also confirmed in the conditions of scenario 4 through

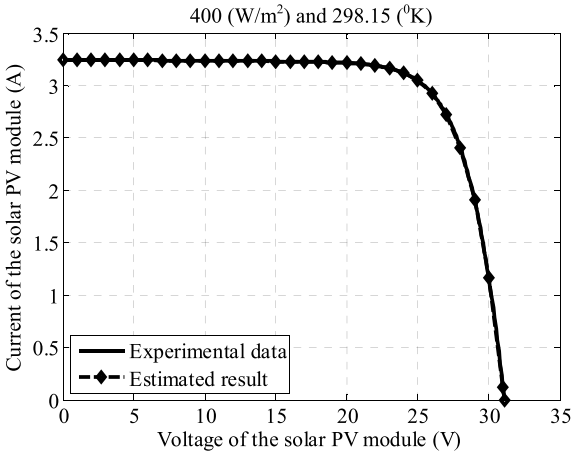

FIGURE 11. $U-I$ characteristics of the PV module obtained by experiment and ISFS algorithm-based estimation with $G = 400$ (W/m^2) and $T = 298.15$ (^{0}K).

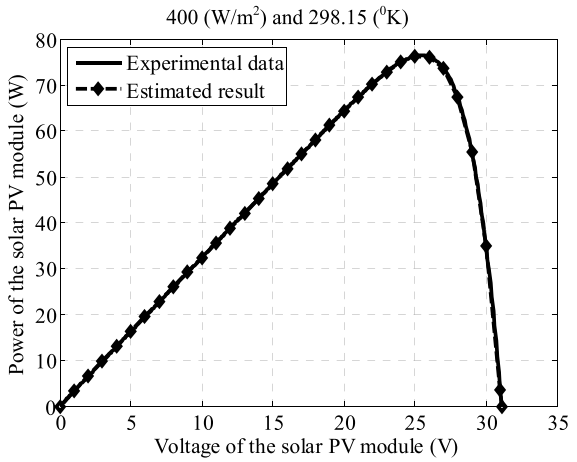

FIGURE 12. $U-P$ characteristics of the PV module obtained by experiment and ISFS algorithm-based estimation with $G = 400$ (W/m^2) and $T = 298.15$ (^{0}K).

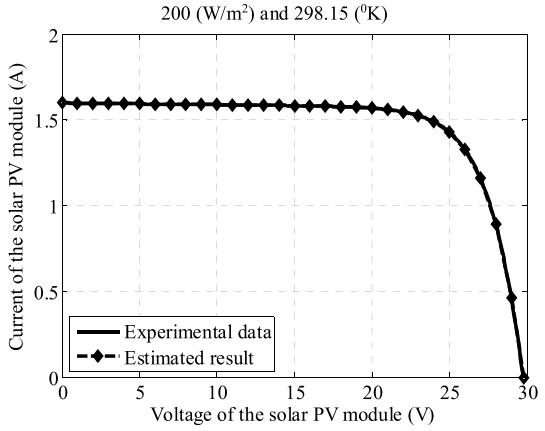

FIGURE 13. $U-I$ characteristics of the PV module obtained by experiment and ISFS algorithm-based estimation with $G = 200$ (W/m^2) and $T = 298.15$ (^{0}K).

the U-I and U-P characteristics Figs. 13-14. Scenario 5 is compared with scenarios 1-4. The comparison shows that $G = 1000$-200 (W/m^2) is decreased and $T = 298.15$ (^{0}K) is constant. The model parameters, I_{ph}, I_0, and a then decrease, the other model parameters, R_{sh} and R_s, increase with the power at the MPP, P_{MPP}, being reduced.

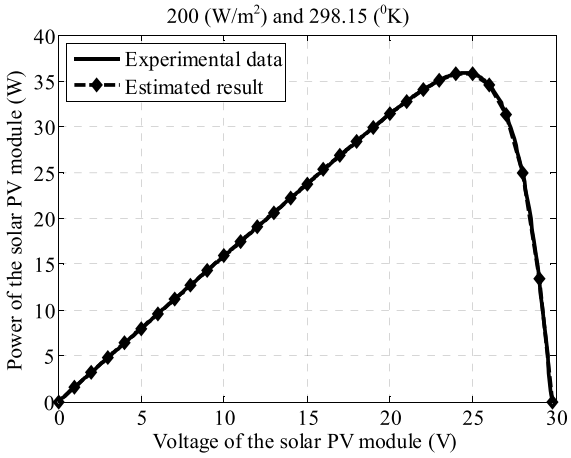

FIGURE 14. $U-P$ characteristics of the PV module obtained by experiment and ISFS algorithm-based estimation with $G = 200$ (W/m^2) and $T = 298.15$ (^{0}K).

When temperature, T, is constant, $T = 298.15$ (^{0}K), and the irradiance, G, is decreased, $G = 1000$-200 (W/m^2); the model parameters, I_{ph}, I_0, and a decreased, whereas the other model parameters, R_{sh} and R_s, increased as shown in Table 10. This shows that the irradiance, G, and the temperature, T, have affected the model parameters, I_{ph}, I_0, a, R_{sh}, and R_s, in the model of the PV module.

Similarly, the MPPs have been influenced by the irradiance, G, and the temperature, T, as well. Then, the MPP moves in the direction that the power at the MPP, P_{MPP}, is reduced as in Table 10.

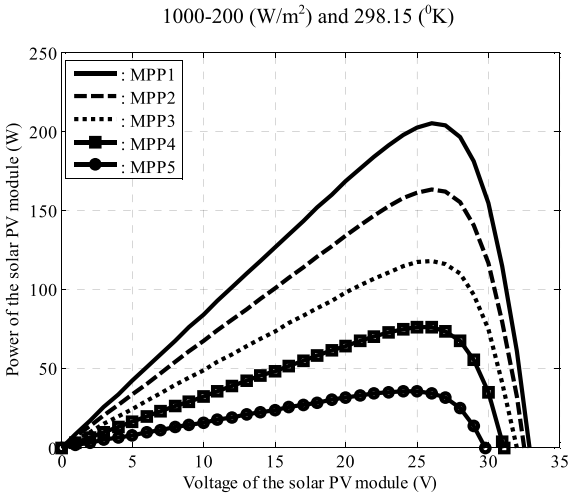

FIGURE 15. MPPs of the PV module estimated by the ISFS algorithm with $G = 1000$-200 (W/m^2) and $T = 298.15$ (^{0}K).

More specifically, Fig. 15 shows the MPPs, MPP_1-MPP_5, of the PV module which are estimated by the ISFS algorithm

where MPP$_1$, $P_{MPP1} = 204.7355$ (W) at $G = 1000$ (W/m^2) and $T = 298.15$ (^{0}K); MPP$_2$, $P_{MPP2} = 161.8392$ (W) at $G = 800$ (W/m^2) and $T = 298.15$ (^{0}K); MPP$_3$, $P_{MPP3} = 118.3574$ (W) at $G = 600$ (W/m^2) and $T = 298.15$ (^{0}K); MPP$_4$, $P_{MPP4} = 75.4100$ (W) at $G = 400$ (W/m^2) and $T = 298.15$ (^{0}K); and MPP$_5$, $P_{MPP5} = 35.5115$ (W) at $G = 200$ (W/m^2) and $T = 298.15$ (^{0}K).

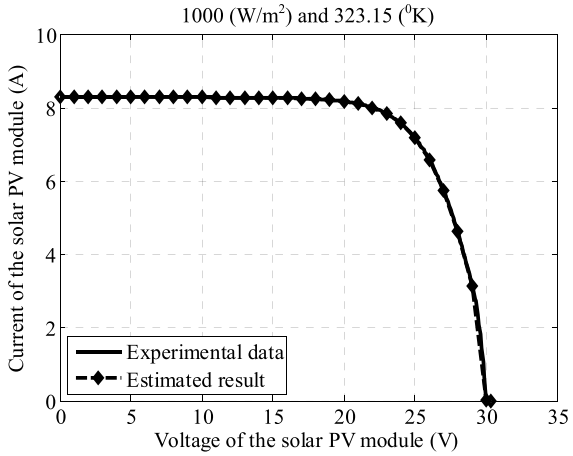

FIGURE 16. $U - I$ characteristics of the PV module obtained by experiment and ISFS algorithm-based estimation with $G = 1000$ (W/m^2) and $T = 323.15$ (^{0}K).

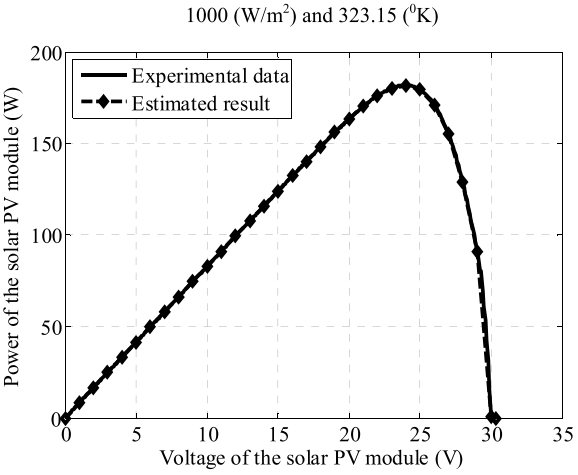

FIGURE 17. $U - P$ characteristics of the PV module obtained by experiment and ISFS algorithm-based estimation with $G = 1000$ (W/m^2) and $T = 323.15$ (^{0}K).

It is assumed that $G = 1000$ (W/m^2) and $T = 323.15$ (^{0}K) in scenario 6, the U-I and U-P characteristics of the PV module obtained by experiment and ISFS algorithm-based estimation are shown in Figs. 16-17. These characteristics confirm the estimation accuracy of the model parameters, $I_{ph} = 8.2880$ (A), $I_0 = 0.2058$ (μA), $R_s = 0.3077$ (Ω), $R_{sh} = 952.1200$ (Ω), $a = 1.3648$; and the MPP, $U_{MPP} = 24.0400$ (V), $I_{MPP} = 7.4969$ (A), $P_{MPP} = 180.2255$ (W) of the PV module by using the ISFS algorithm.

Scenario 6 of $G = 1000$ (W/m^2) and $T = 323.15$ (^{0}K) is compared with scenario 1. The comparison shows that $G = 1000$ (W/m^2) is constant and $T = 298.15$-323.15 (^{0}K) is increased. The model parameters, I_{ph}, I_0 and a, increase as well as the other model parameters, R_{sh} and R_s, and the power at the MPP, P_{MPP}, is reduced.

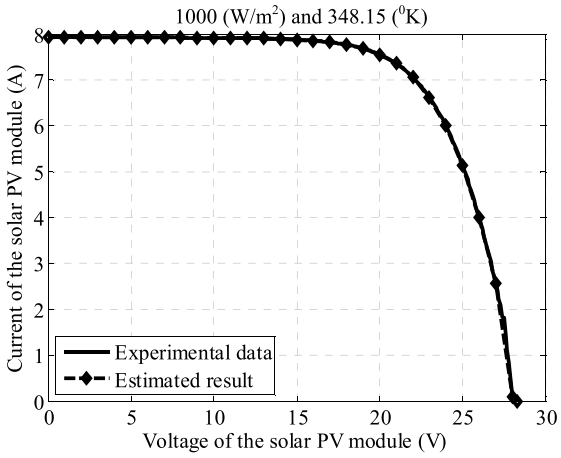

FIGURE 18. $U - I$ characteristics of the PV module obtained by experiment and ISFS algorithm-based estimation with $G = 1000$ (W/m^2) and $T = 348.15$ (^{0}K).

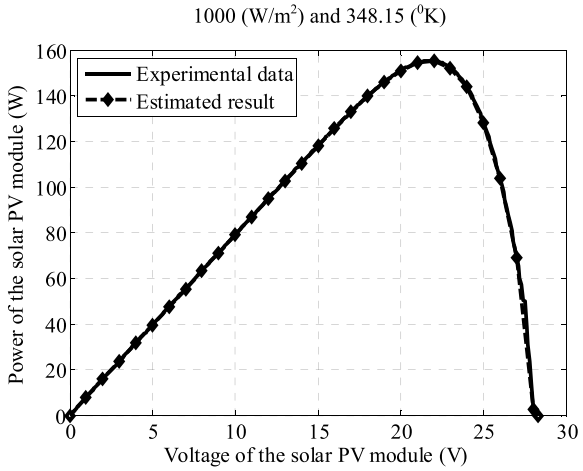

FIGURE 19. $U - P$ characteristics of the PV module obtained by experiment and ISFS algorithm-based estimation with $G = 1000$ (W/m^2) and $T = 348.15$ (^{0}K).

For scenario 7, the U-I and U-P characteristics of the PV module obtained by experiment and ISFS algorithm-based estimation are shown in Figs. 18-19. These characteristics validate the estimation accuracy of the model parameters, $I_{ph} = 8.3770$ (A), $I_0 = 0.2176$ (μA), $R_s = 0.4308$ (Ω), $R_{sh} = 953.7500$ (Ω), $a = 1.3921$; and the MPP, $U_{MPP} = 20.9641$ (V), $I_{MPP} = 7.3199$ (A), $P_{MPP} = 153.4551$ (W) of the PV module by using the ISFS algorithm.

Scenario 7 is then compared with scenarios 1 and 6. This comparison is where $G = 1000$ (W/m^2) is constant and $T = 298.15$-348.15 (^{0}K) is increased. The model parameters, I_{ph}, I_0, and a, and the other model parameters, R_{sh} and R_s, increase, and the power at the MPP, P_{MPP}, is reduced.

The above analyses show when the irradiance, $G = 1000$ (W/m^2), is constant and the temperature, $T = 298.15$-348.15 (^{0}K), is increased, the model parameters, I_{ph}, I_0, and a, and the other model parameters, R_{sh} and R_s, also increase as shown in Table 10. Then, the MPP is moved in the direction that the power at the MPP, P_{MPP}, is reduced as shown in Table 10.

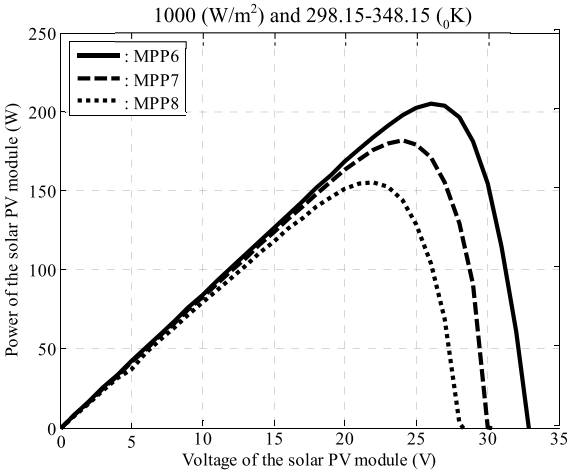

FIGURE 20. MPPs of the PV module estimated by the ISFS algorithm with $G = 1000$ (W/m^2) and $T = 298.15$-348.15 (^{0}K).

More specifically, Fig. 20 shows the MPPs, MPP_6-MPP_8 of the PV module which are estimated by the ISFS algorithm where the MPP_6, $P_{MPP6} = 204.7355$ (W) at $G = 1000$ (W/m^2) and $T = 298.15$ (^{0}K); MPP_7, $P_{MPP7} = 180.2255$ (W) at $G = 1000$ (W/m^2) and $T = 323.15$ (^{0}K); and MPP_8, $P_{MPP8} = 153.4551$ (W) at $G = 1000$ (W/m^2) and $T = 348.15$ (^{0}K). From Figs. 15 and 20, it is realized that the power of the PV module at the MPP is decreased when the irradiance, G, is decreased and the temperature, T, is constant. This is the same when the irradiance, G, is constant and the temperature, T, is increased. Table 11 shows the effect of the irradiance, G, and the temperature, T, on the power, P_{MPP}, achieved at the MPP of the PV module.

TABLE 11. Effect of the irradiance and the temperature on the power at the MPP of The PV module.

No.	Irradiance, G(W/m^2)	Temperature, T(^{0}K)	Power at the MPP, P_{MPP} (W)
1	Constant (-)	Decreased (↓)	Increased (↑)
2	Constant (-)	Increased (↑)	Decreased (↓)
3	Decreased (↓)	Constant (-)	Decreased (↓)
4	Decreased (↓)	Decreased (↓)	Decreased (↓)
5	Increased (↑)	Constant (-)	Increased (↑)
6	Increased (↑)	Increased (↑)	Increased (↑)

When the irradiance, G, is constant, the power, P_{MPP}, at the MPP is inversely proportional to the temperature, T (cases 1-2); and when the temperature, T, is constant, the power, P_{MPP}, at the MPP is directly proportional to the irradiance, G (cases 3 and 5). When both the irradiance, G, and the temperature, T, are decreased, the power, P_{MPP}, at the MPP is decreased (case 4); and when both the irradiance, G, and the temperature, T, are increased, the power, P_{MPP}, at the MPP increases (case 6). This observation is very useful for predicting the achieved power at the MPP, P_{MPP}, under various atmospheric conditions.

TABLE 12. Powers obtained by experiment and The PSO, IPSO, SFS, and ISFS algorithm-based estimations of The PV module with $G = 1000$ (W/m^2)and $T = 298.15$ (^{0}K).

Data	Experimental power (W)	Estimated power (W)			
		PSO	IPSO	SFS	ISFS
1	0.3336	0.2961	0.3114	0.3155	0.3335
2	8.5627	7.6753	8.0256	8.0501	8.5595
3	16.7868	15.0574	15.7524	15.7851	16.7788
4	24.9853	22.1800	23.2470	23.6161	24.9740
5	33.1709	29.5078	31.1470	31.3466	33.1549
6	39.9349	35.5879	37.4014	37.7556	39.9203
7	48.8115	43.8567	45.5136	46.1311	48.8026
8	56.9789	50.1879	53.3240	53.8145	56.9721
9	65.1486	57.8754	60.8102	61.5465	65.1382
10	73.0495	65.7189	68.1423	69.0813	73.0241
11	81.1776	72.2587	75.8143	76.7912	81.1476
12	89.3920	79.8547	84.0061	84.4675	89.3678
13	96.7264	85.5974	90.2479	91.4460	96.7162
14	104.7026	92.5785	98.1934	98.9394	104.6673
15	112.8109	100.0257	105.8031	106.6306	112.7858
16	120.6972	107.5178	112.6871	114.0895	120.6471
17	128.7872	114.2873	120.8011	121.7903	128.7428
18	136.5591	121.8971	127.5691	129.0577	136.5213
19	144.7159	129.4751	135.8230	136.5756	144.6714
20	152.4258	135.2897	142.8014	144.2043	152.3844
21	160.1495	142.8751	149.2173	151.3124	160.1242
22	168.1763	149.8532	157.1573	158.9622	168.1252
23	175.7969	157.8236	163.5813	166.1128	175.7387
24	182.1966	161.5873	170.3410	172.1875	182.1143
25	190.2547	170.5239	177.3141	179.7079	190.1674
26	197.2389	175.8435	183.9914	186.3890	197.1571
27	202.6243	179.0811	188.5671	191.4008	202.5655
28	204.7370	181.7075	192.1002	193.4567	204.7011
29	200.2507	178.5783	186.1569	189.2963	200.1679
30	188.1281	168.7122	175.1473	177.1118	188.0547
31	162.8831	143.8433	152.8420	153.2469	162.8513
32	118.7673	105.2147	111.1473	112.3251	118.7360
33	68.8374	60.8766	64.7169	65.1305	68.8181
34	14.4879	12.8791	13.5154	13.7006	14.4853

The estimation precision of the model parameters and MPPs of the PV module are also shown specifically through powers obtained experimentally and the PSO, IPSO, SFS and ISFS algorithm-based estimation of the PV module with $G = 1000$ (W/m^2) and $T = 298.15$ (^{0}K) in Tables 12-13. Table 12 contains the powers obtained by the experiments and the PSO, IPSO, SFS and ISFS algorithm-based estimations of the PV module with $G = 1000$ (W/m^2) and $T = 298.15$ (^{0}K). From these achieved powers, a comparison is performed between the powers obtained experimentally and the PSO, IPSO, SFS and ISFS algorithm-based estimations of the PV module with $G = 1000$ (W/m^2) and $T = 298.15$ (^{0}K). It is observed that the characteristic of the ISFS algorithm-based estimated power nearly matches the characteristic of the experimental power in Fig. 21. The characteristics of the SFS and IPSO algorithms-based estimated powers have almost the same differences compared with the characteristic

TABLE 13. Error percentages of the obtained powers between experiment and the PSO, IPSO, SFS, AND ISFS algorithm-based estimations of the PV module with G =1000 (W/m^2) and T = 298.15 (^{0}K).

Data	Error percentage of estimated power (%)			
	PSO	IPSO	SFS	ISFS
1	11.24	6.65	5.42	0.025
2	10.36	6.27	5.99	0.038
3	10.30	6.16	5.97	0.047
4	11.23	6.96	5.48	0.045
5	11.04	6.10	5.50	0.048
6	10.89	6.34	5.46	0.037
7	10.15	6.76	5.49	0.018
8	11.92	6.41	5.55	0.012
9	11.16	6.66	5.53	0.016
10	10.04	6.72	5.43	0.035
11	10.99	6.61	5.40	0.037
12	10.67	6.02	5.51	0.027
13	11.51	6.70	5.46	0.011
14	11.58	6.22	5.50	0.034
15	11.33	6.21	5.48	0.022
16	10.92	6.64	5.47	0.041
17	11.26	6.20	5.43	0.034
18	10.74	6.58	5.49	0.027
19	10.53	6.15	5.63	0.031
20	11.24	6.31	5.39	0.027
21	10.79	6.83	5.52	0.016
22	10.90	6.55	5.48	0.030
23	10.22	6.95	5.51	0.033
24	11.31	6.51	5.49	0.045
25	10.37	6.80	5.54	0.046
26	10.85	6.72	5.50	0.041
27	11.62	6.94	5.54	0.029
28	11.25	6.17	5.51	0.018
29	10.82	7.04	5.47	0.041
30	10.32	6.90	5.86	0.039
31	11.69	6.16	5.92	0.020
32	11.41	6.42	5.42	0.026
33	11.56	5.99	5.38	0.028
34	11.10	6.71	5.43	0.018

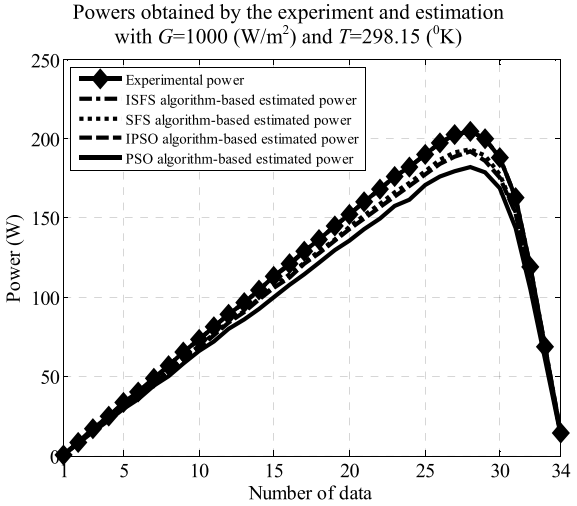

FIGURE 21. Powers obtained by experiment and PSO, IPSO, SFS, and ISFS algorithm-based estimations of the PV module with G = 1000 (W/m2) and T = 298.15 (^{0}K).

of the experimental power. The characteristic of the PSO algorithm-based estimated power has the largest difference compared with the characteristic of the experimental power.

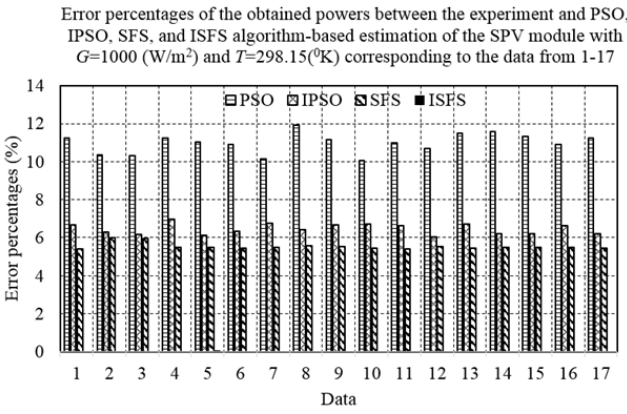

FIGURE 22. Error percentages of the obtained powers between experiment and the PSO, IPSO, SFS and ISFS algorithm-based estimations of data from 1 to 17 of the PV module with G = 1000 (W/m^2) and T = 298.15 (^{0}K).

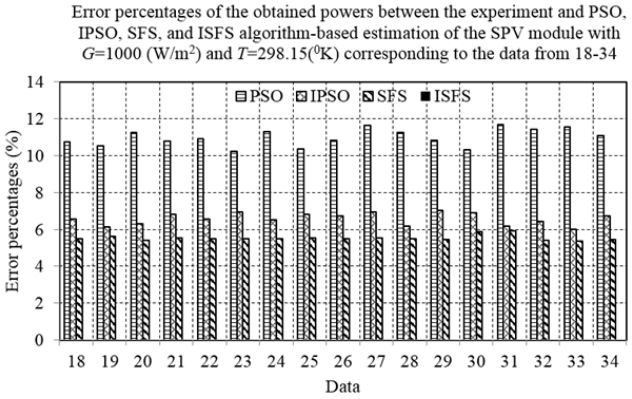

FIGURE 23. Error percentages of the obtained powers between experiment and the PSO, IPSO, SFS and ISFS algorithm-based estimations of data from 18 to 34 of the PV module with G = 1000 (W/m^2) and T = 298.15 (^{0}K).

Figs. 22-23 are the error percentages of the obtained powers of the PV module with G = 1000 (W/m^2) and T = 298.15 (^{0}K) between the experiment and the PSO, IPSO, SFS and ISFS algorithm-based estimations of data from 1 to 17 and from 18 to 34 respectively. It is realized that the error percentages of the obtained powers of the PV module with G = 1000 (W/m^2) and T = 298.15 (^{0}K) between the experiment and the ISFS algorithm-based estimation have the smallest error percentages when compared with the error percentages of the SFS, IPSO and PSO algorithm-based estimations whereas the PSO algorithm-based results have the largest error percentages. For more detail, Table 13 shows that the error percentages of the obtained powers are always less than 0.048% with the ISFS algorithm whereas the errors are always greater than 5.38%, 5.99%, and 10.04% with the SFS, IPSO and PSO algorithms respectively. This comparison further confirms the accuracy of the ISFS algorithm-estimated parameters, as well as the significant improvement of the ISFS algorithm-based estimation results compared to the PSO, IPSO and SFS algorithm-based estimation results.

This shows the effectiveness of improvements in the proposed procedures of initializing solutions, creating a new solution and updating the solution based on chaotic maps.

TABLE 14. Convergence of The PSO, IPSO, SFS, and ISFS algorithms in the estimation application of the model parameters and MPP with $G = 1000$ (W/m^2) and $T = 298.15$ (^{0}K).

Algorithm	Convergence value	Convergence iteration number
PSO	0.0088	538
IPSO	0.0036	426
SFS	0.0021	404
ISFS	0.000062	216

Table 14 shows the convergence value and iteration number of the PSO, IPSO, SFS and ISFS algorithms in the estimation application of the model parameters and MPP with the scenario of $G = 1000$ (W/m^2) and $T = 298.15$ (^{0}K). In this scenario, the convergence value and iteration number are significantly improved when utilizing the ISFS algorithm in the estimation application. The convergence value of the ISFS algorithm, 0.000062, is better than the convergence values, 0.0021, 0.0036, and 0.0088, of the SFS, IPSO and PSO algorithms respectively. Additionally, the convergence iteration number of the ISFS algorithm, 216, is also better than the convergence iteration numbers, 404, 426 and 538, of the SFS, IPSO and PSO algorithms respectively.

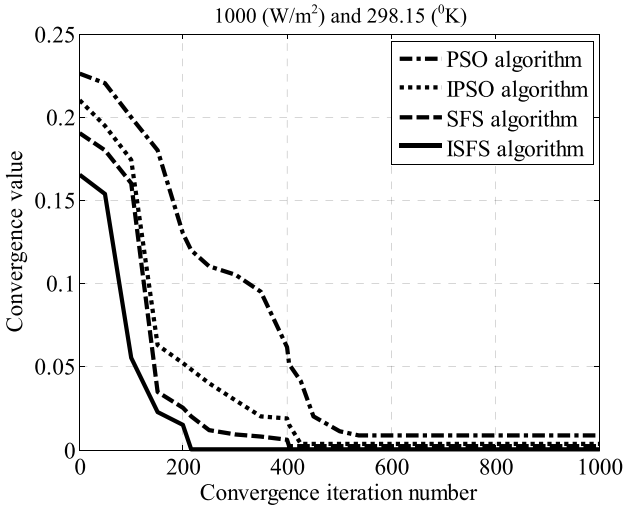

FIGURE 24. Convergence characteristics of the PSO, IPSO, SFS and ISFS algorithms in the estimation application of the model parameters and MPP of the PV module with $G = 1000$ (W/m^2) and $T = 298.15$ (^{0}K).

Fig. 24 shows that the solution initialization of the ISFS algorithm is better than that of the SFS, IPSO and PSO algorithms. This confirms the effectiveness of the proposal in the sine map-based initialization procedure of solutions. The improvements are also shown in the procedures of creating a new solution and updating the solution to retain the balance between the exploration and exploitation of globally optimal solutions.

TABLE 15. Convergence of The PSO, IPSO, SFS, and ISFS algorithms in the estimation application of the model parameters and MPP with $G = 800$ (W/m^2) and $T = 298.15$ (^{0}K).

Algorithm	Convergence value	Convergence iteration number
PSO	0.0092	529
IPSO	0.0032	421
SFS	0.0026	415
ISFS	0.000058	207

In the scenario with $G = 800$ (W/m^2) and $T = 298.15$ (^{0}K), Table 15 shows the convergence value and iteration number of the PSO, IPSO, SFS and ISFS algorithms in the estimation application of the model parameters and MPP. The convergence value of the ISFS algorithm is 0.000058 compared with the convergence values, 0.0026, 0.0032, and 0.0092 of the SFS, IPSO and PSO algorithms respectively. Furthermore, the convergence iteration number of the ISFS algorithm is 207 compared with the convergence iteration numbers, 415, 421 and 529 of the SFS, IPSO and PSO algorithms respectively. The comparisons show that the convergence of the ISFS algorithm is significantly improved in the estimation application of the model parameters and MPP with $G = 800$ (W/m^2) and $T = 298.15$ (^{0}K) because of the improved procedures of initializing solutions, creating a new solution, and updating the solution. The solution initialization of the ISFS algorithm is better than that of the SFS, IPSO and PSO algorithms through the sine map, Fig. 25. This is one of the advantages of the ISFS algorithm which is that the convergence iteration number is always less than that of the SFS, IPSO and PSO algorithms.

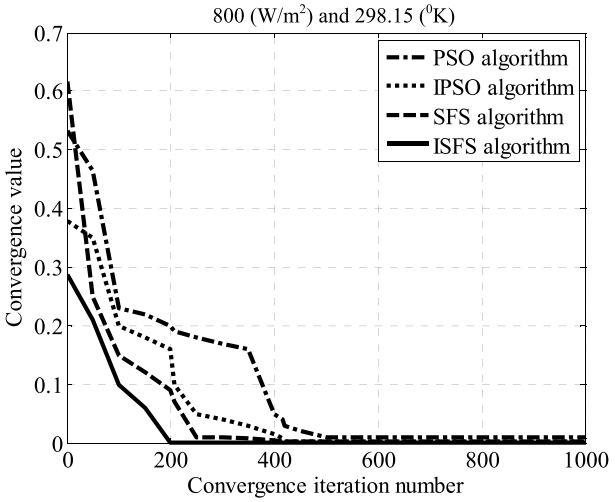

FIGURE 25. Convergence characteristics of the PSO, IPSO, SFS and ISFS algorithms in the estimation application of the model parameters and MPP of the PV module with $G = 800$ (W/m^2) and $T = 298.15$ (^{0}K).

Similarly, when $G = 600$ (W/m^2) and $T = 298.15$ (^{0}K), the convergence characteristics of the PSO, IPSO, SFS and ISFS algorithms in the estimation application of the model parameters and MPP are shown in Fig. 26. This shows that

TABLE 16. Convergence of The PSO, IPSO, SFS, and ISFS algorithms in the estimation application of the model parameters and MPP with $G = 600$ (W/m^2) and $T = 298.15$ (^{0}K).

Algorithm	Convergence value	Convergence iteration number
PSO	0.0090	534
IPSO	0.0034	425
SFS	0.0025	410
ISFS	0.000060	212

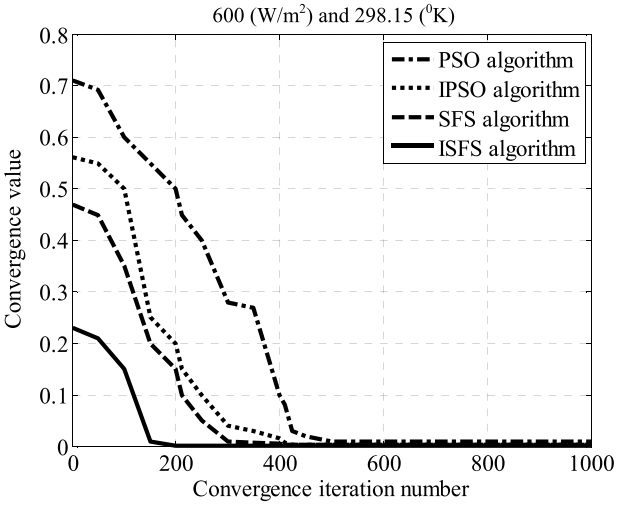

FIGURE 26. Convergence characteristics of the PSO, IPSO, SFS, and ISFS algorithms in the estimation application of the model parameters and MPP of the PV module with $G = 600$ (W/m^2) and $T = 298.15$ (^{0}K).

the convergence characteristic of the ISFS algorithm is better than that of the SFS, IPSO and PSO algorithms, especially in the solution initialization. Table 16 shows the convergence value and iteration number of the PSO, IPSO, SFS and ISFS algorithms in the estimation application of the model parameters and MPP with $G = 600$ (W/m^2) and $T = 298.15$ (^{0}K). The convergence value of the ISFS algorithm, 0.000060, is better than the convergence values, 0.0025, 0.0034 and 0.0090 of the SFS, IPSO and PSO algorithms respectively. The convergence iteration number of the ISFS algorithm, 212, is better than the convergence iteration numbers, 410, 425 and 534 of the SFS, IPSO and PSO algorithms respectively. Both the convergence value and iteration number of the ISFS algorithm are better than those of the SFS, IPSO and PSO algorithms.

This is similar to the convergence characteristics for the scenarios of $G = 400$ (W/m^2) and $T = 298.15$ (^{0}K), Fig. 27, and $G = 200$ (W/m^2) and $T = 298.15$ (^{0}K), Fig. 28. The above scenarios assumed that G is decreased and T is constant. The convergence characteristics of the ISFS algorithm with the sine map-based solution initialization are also better than the convergence characteristics of the SFS, IPSO and PSO algorithms. This shows that the performance of the ISFS algorithm is not dependent on the conditions of G and T. It is always better than the performance of the SFS, IPSO and PSO algorithms.

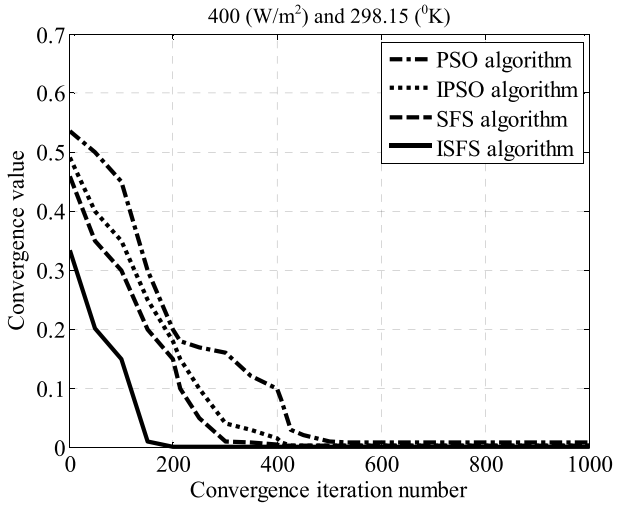

FIGURE 27. Convergence characteristics of the PSO, IPSO, SFS and ISFS algorithms in the estimation application of the model parameters and MPP of the PV module with $G = 400$ (W/m^2) and $T = 298.15$ (^{0}K).

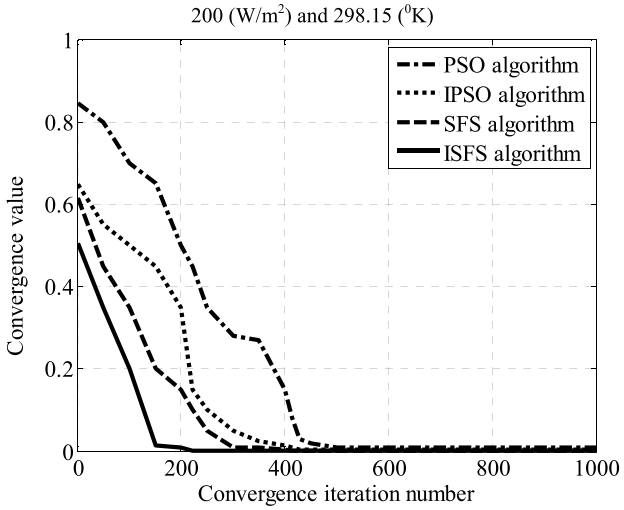

FIGURE 28. Convergence characteristics of the PSO, IPSO, SFS and ISFS algorithms in the estimation application of the model parameters and MPP of the PV module with $G = 200$ (W/m^2) and $T = 298.15$ (^{0}K).

TABLE 17. Convergence of The PSO, IPSO, SFS, and ISFS algorithms in the estimation application of the model parameters and MPP with. $G = 400$ (W/m^2) and $T = 298.15$ (^{0}K).

Algorithm	Convergence value	Convergence iteration number
PSO	0.0089	536
IPSO	0.0035	427
SFS	0.0023	407
ISFS	0.000061	214

Table 17 shows the convergence value and iteration number of the PSO, IPSO, SFS and ISFS algorithms in the estimation application of the model parameters and MPP with $G = 400$ (W/m^2) and $T = 298.15$ (^{0}K). It shows that the convergence value of the ISFS algorithm, 0.000061, is better than the convergence values, 0.0023, 0.0035 and

0.0089, of the SFS, IPSO and PSO algorithms respectively. The convergence iteration number of the ISFS algorithm, 214, is better than the convergence iteration numbers, 407, 427 and 536, of the SFS, IPSO, and PSO algorithms respectively.

TABLE 18. Convergence of The PSO, IPSO, SFS, and ISFS algorithms in the estimation application of the model parameters and MPP with. G = 200 (W/m^2) and T = 298.15 (^{0}K).

Algorithm	Convergence value	Convergence iteration number
PSO	0.0091	537
IPSO	0.0037	429
SFS	0.0022	413
ISFS	0.000073	221

Moreover, Table 18 shows the convergence value and iteration number of the PSO, IPSO, SFS and ISFS algorithms in the estimation application of the model parameters and MPP with $G = 200$ (W/m^2) and $T = 298.15$ (^{0}K). As with the scenarios of $G = 400$ (W/m^2), 600 (W/m^2), 800 (W/m^2) and 1000 (W/m^2), the convergence value of the ISFS algorithm, 0.000073, is better than the convergence values, 0.0022, 0.0037 and 0.0091, of the SFS, IPSO and PSO algorithms respectively. In addition, the convergence iteration number of the ISFS algorithm, 221, is better than the convergence iteration numbers, 413, 429 and 537, of the SFS, IPSO and PSO algorithms respectively.

In another scenario, the irradiance, G, is assumed to increase to 1000 (W/m^2) which is compared with the previous scenarios of 800 (W/m^2), 600 (W/m^2), 400 (W/m^2) and 200 (W/m^2), as well as the temperature, T, is assumed to increase to 323.15 (^{0}K) compared with the previous scenario of 298.15 (^{0}K).

TABLE 19. Convergence of The PSO, IPSO, SFS, and ISFS algorithms in the estimation application of the model parameters and MPP with. G = 1000 (W/m^2) and T = 323.15 (^{0}K).

Algorithm	Convergence value	Convergence iteration number
PSO	0.0087	546
IPSO	0.0028	431
SFS	0.0019	423
ISFS	0.000055	219

Table 19 shows the convergence value and iteration number of the PSO, IPSO, SFS and ISFS algorithms in the estimation application of the model parameters and MPP with $G = 1000$ (W/m^2) and $T = 323.15$ (^{0}K). The convergence value of the ISFS algorithm, 0.000055 is better than the convergence values, 0.0019, 0.0028 and 0.0087, of the SFS, IPSO and PSO algorithms respectively. Additionally, the convergence iteration number of the ISFS algorithm, 219, is better than the convergence iteration numbers, 423, 431 and 546, of the SFS, IPSO and PSO algorithms respectively. This is also shown through the convergence characteristics of the ISFS, SFS, IPSO and PSO algorithms, Fig. 29. It is realized that the effectiveness of the improved procedures of initializing solutions, creating a new solution and updating the solution is re-confirmed, especially the procedure of sine map-based solution initialization.

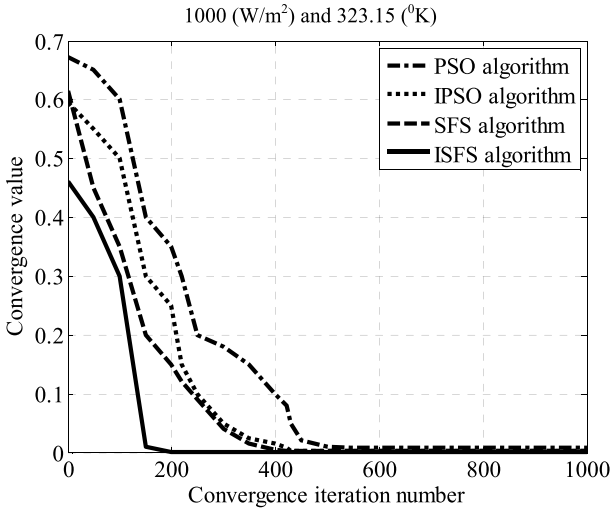

FIGURE 29. Convergence characteristics of the PSO, IPSO, SFS, and ISFS algorithms in the estimation application of the model parameters and MPP of the PV module with G = 1000 (W/m^2) and T = 323.15 (^{0}K).

TABLE 20. Convergence of The PSO, IPSO, SFS and ISFS Algorithms in the estimation application of the model parameters and MPP with G = 1000 (W/m^2) and T = 348.15 (^{0}K).

Algorithm	Convergence value	Convergence iteration number
PSO	0.0096	521
IPSO	0.0043	418
SFS	0.0038	397
ISFS	0.000076	206

An additional scenario is presented to validate the proposal where the irradiance, G, is assumed to increase to 1000 (W/m^2) compared with the previous scenarios of 800 (W/m^2), 600 (W/m^2), 400 (W/m^2) and 200 (W/m^2), and the temperature, T, is assumed to increase to 348.15 (^{0}K) compared with the previous scenarios of 323.15 (^{0}K) and 298.15 (^{0}K). Table 20 shows the convergence value and iteration number of the PSO, IPSO, SFS and ISFS algorithms in the estimation application of the model parameters and MPP with $G = 1000$ (W/m^2) and $T = 348.15$ (^{0}K). The convergence value of the ISFS algorithm, 0.000076, is better than the convergence values, 0.0038, 0.0043 and 0.0096, of the SFS, IPSO and PSO algorithms respectively. Moreover, the convergence iteration number of the ISFS algorithm, 206, is better than the convergence iteration numbers, 397, 418 and 512, of the SFS, IPSO and PSO algorithms respectively. This improvement is also shown through the convergence characteristics of the ISFS, SFS, IPSO and PSO algorithms, Fig. 30.

The achieved numerical results show the convergence ability of the ISFS, SFS, IPSO and PSO algorithms in the proposed estimation application of the model parameters and MPPs of the PV module with G = 200-1000 (W/m^2) and

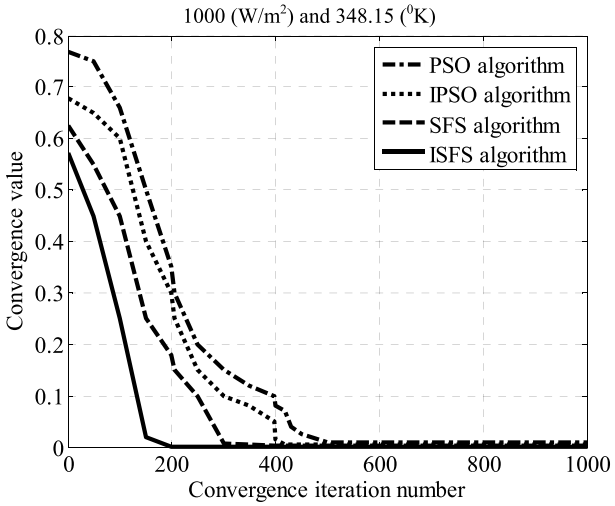

FIGURE 30. Convergence characteristics of the PSO, IPSO, SFS, and ISFS algorithms in the estimation application of the model parameters and MPP of the PV module with $G = 1000$ (W/m^2) and $T = 348.15$ (^{0}K).

$T = 298.15$-348.15 (^{0}K). It is realized that the performance, in terms of the convergence value and iteration number, of the ISFS algorithm is always better than that of the SFS, IPSO and PSO algorithms because of the chaotic map-based modifications in the solution initialization, the procedure of creating a new solution and the procedure of updating the solution. The improvement is the same with various atmospheric conditions of the irradiance and the temperature. This also re-confirms the estimation accuracy of the model parameters and MPPs of the PV module with various atmospheric conditions of the irradiance and the temperature by utilizing the ISFS algorithm.

V. CONCLUSION

A novel approach to simultaneously determine the model parameters and MPPs of the PV module has been successfully developed using the ISFS algorithm. The ISFS algorithm improves the procedures for initializing solutions, creating a new solution and updating the solution in the ISFS algorithm. Specifically, the logarithmic function is modified into the exponential function in the standard deviation of the diffusion technique for improving the exploration ability efficiently in the solution search space. Simultaneously, the uniform distribution is transformed into the sine map in both the diffusion and update techniques for enhancing the performance of the ISFS algorithm. The ISFS algorithm has been shown to perform extremely well for the estimation problem of the model parameters and MPPs of the PV module in the PV power generation system under various atmospheric conditions of irradiance and temperature.

The numerical results indicate that the estimation results of the model parameters and MPPs of the PV module when using the ISFS algorithm are always better than those produced by the SFS, IPSO and PSO algorithms in various scenarios.

The error percentages of the ISFS algorithm-based power estimations are significantly less compared to the ones obtained from the SFS, IPSO and PSO algorithms.

In addition, the estimation results of the model parameters and the MPP of the PV module are also confirmed through the performance of the ISFS, SFS, IPSO and PSO algorithms. The performance of the ISFS algorithm is always better than that of the SFS, IPSO and PSO algorithms in the estimation of the model parameters and the MPP of the PV module in terms of the convergence value and iteration number.

REFERENCES

[1] D. C. Huynh and M. W. Dunnigan, "Development and comparison of an improved incremental conductance algorithm for tracking the MPP of a solar PV panel," *IEEE Trans. Sustain. Energy*, vol. 7, no. 4, pp. 1421–1429, Oct. 2016.

[2] D. C. Huynh, L. D. Ho, and M. W. Dunnigan, "Parameter estimation of solar photovoltaic arrays using an artificial bee colony algorithm," in *Proc. 5th Int. Conf. Green Technol. Sustain. Develop., Adv. Intell. Syst. Comput.*, vol. 1284, 2020, pp. 281–292.

[3] A. A. Teyabeen, N. B. Elhatmi, A. A. Essnid, and A. E. Jwaid, "Parameters estimation of solar PV modules based on single-diode model," in *Proc. 11th Int. Renew. Energy Congr. (IREC)*, 2020, pp. 1–6.

[4] D. C. Huynh, L. D. Ho, and M. W. Dunnigan, "Unknown parameter estimation of a detailed solar PV cell model," in *Proc. IEEE Region 10 Conf. (TENCON)*, Nov. 2020, pp. 1–5.

[5] A. A. Z. Diab, H. M. Sultan, T. D. Do, O. M. Kamel, and M. A. Mossa, "Coyote optimization algorithm for parameters estimation of various models of solar cells and PV modules," *IEEE Access*, vol. 8, pp. 111102–111140, 2020.

[6] J. Aller, J. Viola, F. Quizhpi, J. Restrepo, A. Ginart, and A. Salazar, "Implicit PV cell parameters estimation used in approximated closed-form model for inverter power control," in *Proc. IEEE Workshop Power Electron. Power Quality Appl. (PEPQA)*, May 2017, pp. 1–6.

[7] K. Ayache, A. Chandra, A. Cheriti, and M. A. Ouameur, "AC dynamic parameters extraction of shaded solar cells based on analytical methods and LMLS algorithm," in *Proc. 44th Annu. Conf. IEEE Ind. Electron. Soc. (IECON)*, Oct. 2018, pp. 1681–1686.

[8] A. Benahmida, N. Maouhoub, H. Sahsah, H. Mokhliss, and K. Rais, "Parameter identification of photovoltaic generators using an analytical approach and iterative method," in *Proc. Int. Conf. Comput. Sci. Renew. Energies (ICCSRE)*, Jul. 2019, pp. 1–5.

[9] U. Jadli, P. Thakur, and R. D. Shukla, "A new parameter estimation method of solar photovoltaic," *IEEE J. Photovolt.*, vol. 8, no. 1, pp. 239–247, Jan. 2018.

[10] I. Nassar-eddine, K. Et-torabi, R. Rmaily, A. Obbadi, Y. Errami, S. Sahnoun, A. E. Fajri, and M. Agunaou, "Parameter identification of multicrystalline modules using two methods and five improved mathematical models," in *Proc. 6th Int. Renew. Sustain. Energy Conf. (IRSEC)*, Dec. 2018, pp. 1–6.

[11] M.-U.-N. Khursheed, M. A. Alghamdi, M. F. N. Khan, A. K. Khan, I. Khan, A. Ahmed, A. T. Kiani, and M. A. Khan, "PV model parameter estimation using modified FPA with dynamic switch probability and step size function," *IEEE Access*, vol. 9, pp. 42027–42044, 2021.

[12] P. Bharadwaj, K. N. Chaudhury, and V. John, "Sequential optimization for PV panel parameter estimation," *IEEE J. Photovolt.*, vol. 6, no. 5, pp. 1261–1268, Sep. 2016.

[13] M. Kumar and D. V. S. K. Rao K, "Modelling and parameter estimation of solar cell using genetic algorithm," in *Proc. Int. Conf. Intell. Comput. Control Syst. (ICCS)*, May 2019, pp. 383–387.

[14] M. Ulaganathan and D. Devaraj, "RGA based optimal parameter estimation of diode model for solar photo-voltaic array emulator development," in *Proc. IEEE Int. Conf. Clean Energy Energy Efficient Electron. Circuit Sustain. Develop. (INCCES)*, Dec. 2019, pp. 1–6.

[15] A. T. Kiani, M. Faisal Nadeem, A. Ahmed, I. A. Sajjad, A. Raza, and I. A. Khan, "Chaotic inertia weight particle swarm optimization (CIW-PSO): An efficient technique for solar cell parameter estimation," in *Proc. 3rd Int. Conf. Comput., Math. Eng. Technol. (iCoMET)*, Jan. 2020, pp. 1–6.

[16] A. T. Kiani, M. F. Nadeem, A. Ahmed, I. A. Sajjad, M. S. Haris, and L. Martirano, "Optimal parameter estimation of solar cell using simulated annealing inertia weight particle swarm optimization (SAIW-PSO)," in *Proc. IEEE Int. Conf. Environ. Electr. Eng. IEEE Ind. Commercial Power Syst. Eur. (EEEIC/ICPS Europe)*, Jun. 2020, pp. 1–6.

[17] K. J. Yu, S. L. Ge, B. Y. Qu, and J. J. Liang, "A modified particle swarm optimization for parameters identification of photovoltaic models," in *Proc. IEEE Congr. Evol. Comput. (CEC)*, Jun. 2019, pp. 1–6.

[18] M. Shahabuddin, M. Asim, and A. Sarwar, "Parameter extraction of a solar PV cell using projectile search algorithm," in *Proc. Int. Conf. Adv. Comput., Commun. Mater. (ICACCM)*, Aug. 2020, pp. 1–6.

[19] A. A. Z. Diab, H. M. Sultan, R. Aljendy, A. S. Al-Sumaiti, M. Shoyama, and Z. M. Ali, "Tree growth based optimization algorithm for parameter extraction of different models of photovoltaic cells and modules," *IEEE Access*, vol. 8, pp. 119668–119687, 2020.

[20] R. Y. Abdelghany, S. Kamel, A. Ramadan, H. M. Sultan, and C. Rahmann, "Solar cell parameter estimation using school-based optimization algorithm," in *Proc. IEEE Int. Conf. Automat./XXIV Congr. Chilean Assoc. Autom. Control (ICA-ACCA)*, Mar. 2021, pp. 1–6.

[21] H. Salimi, "Stochastic fractal search: A powerful metaheuristic algorithm," *Knowl.-Based Syst.*, vol. 75, pp. 1–18, Feb. 2015.

[22] T. A. Z. Rahman, "Parametric modelling of twin rotor system using chaotic fractal search algorithm," in *Proc. 7th IEEE Control Syst. Graduate Res. Colloq. (ICSGRC)*, Aug. 2016, pp. 34–39.

[23] H. Mosbah and M. El-Hawary, "Power system tracking state estimation based on stochastic fractal search technique under sudden load changing conditions," in *Proc. IEEE Can. Conf. Electr. Comput. Eng. (CCECE)*, May 2016, pp. 1–6.

[24] H. Mosbah and M. E. El-Hawary, "Power system tracking state estimation based on stochastic fractal search technique under bad measurements conditions," in *Proc. IEEE Electr. Power Energy Conf. (EPEC)*, Oct. 2016, pp. 1–6.

[25] H. Mosbah and M. E. El-Hawary, "Optimized neural network parameters using stochastic fractal technique to compensate Kalman filter for power system-tracking-state estimation," *IEEE Trans. Neural Netw. Learn. Syst.*, vol. 30, no. 2, pp. 379–388, Feb. 2019.

[26] R. K. Khadanga, V. Kumar, A. Kumar, and S. Padhy, "Robust frequency control in an islanded microgrid: A novel stochastic fractal search algorithm approach," in *Proc. 14th IEEE India Council Int. Conf. (INDICON)*, Dec. 2017, pp. 1–6.

[27] M. I. Alomoush, "Optimal combined heat and power economic dispatch using stochastic fractal search algorithm," *J. Modern Power Syst. Clean Energy*, vol. 8, no. 2, pp. 276–286, 2020.

[28] I. Khanam and G. Parmar, "Application of SFS algorithm in control of DC motor and comparative analysis," in *Proc. 4th IEEE Uttar Pradesh Sect. Int. Conf. Electr., Comput. Electron. (UPCON)*, Oct. 2017, pp. 256–261.

[29] T. A. Z. Rahman, A. As'Arry, N. A. A. Jalil, and R. M. K. R. Ahmad, "Chaotic fractal search algorithm for global optimization with application to control design," in *Proc. IEEE Symp. Comput. Appl. Ind. Electron. (ISCAIE)*, Apr. 2017, pp. 111–116.

[30] I. G. N. A. I. Mandala, Franky, and Y. Y. Nazaruddin, "Optimization of two degree of freedom PID controller for quadrotor with stochastic fractal search algorithm," in *Proc. IEEE Conf. Control Technol. Appl. (CCTA)*, Aug. 2019, pp. 1062–1067.

[31] S. Bandong, M. R. Miransyahputra, Y. Setiaji, Y. Y. Nazaruddin, P. I. Siregar, and E. Joelianto, "Optimization of gantry crane PID controller based on PSO, SFS, and FPA," in *Proc. 60th Annu. Conf. Soc. Instrum. Control Eng. Jpn. (SICE)*, 2021, pp. 1–6.

[32] W. Li, S. Sun, J. Li, and Y. Hu, "Stochastic fractal search algorithm and its application in path planning," in *Proc. IEEE CSAA Guid., Navigat. Control Conf. (CGNCC)*, Aug. 2018, pp. 1–5.

[33] A. A. Abdelhamid, E.-S.-M. El-Kenawy, B. Alotaibi, G. M. Amer, M. Y. Abdelkader, A. Ibrahim, and M. M. Eid, "Robust speech emotion recognition using CNN+LSTM based on stochastic fractal search optimization algorithm," *IEEE Access*, vol. 10, pp. 49265–49284, 2022.

[34] D. C. Huynh, T. A. T. Nguyen, M. W. Dunnigan, and M. A. Mueller, "Maximum power point tracking of solar photovoltaic panels using advanced perturbation and observation algorithm," in *Proc. IEEE 8th Conf. Ind. Electron. Appl. (ICIEA)*, Jun. 2013, pp. 864–869.

[35] D. C. Huynh and M. W. Dunnigan, "Maximum power point tracking using an adaptive perturbation and observation algorithm for a grid-connected solar photovoltaic system," *Int. J. Grid Distrib. Comput.*, vol. 8, no. 3, pp. 97–110, Jun. 2015.

[36] L. Assiya, D. Aziz, and H. Ahmed, "Comparative study of P&O and INC MPPT algorithms for DC-DC converter based PV system on MATLAB/SIMULINK," in *Proc. IEEE 2nd Int. Conf. Electron., Control, Optim. Comput. Sci. (ICECOCS)*, Dec. 2020, pp. 1–6.

[37] U. Chauhan, A. Rani, V. Singh, and B. Kumar, "A modified incremental conductance maximum power point technique for standalone PV system," in *Proc. 7th Int. Conf. Signal Process. Integr. Netw. (SPIN)*, Feb. 2020, pp. 61–64.

[38] S. Samal, P. K. Barik, and S. K. Sahu, "Extraction of maximum power from a solar PV system using fuzzy controller based MPPT technique," in *Proc. Technol. Smart-City Energy Secur. Power (ICSESP)*, Mar. 2018, pp. 1–6.

[39] T. Radjai, L. Rahmani, S. Mekhilef, and J. P. Gaubert, "Implementation of a modified incremental conductance MPPT algorithm with direct control based on a fuzzy duty cycle change estimator using dSPACE," *Sol. Energy*, vol. 110, pp. 325–337, Dec. 2014.

[40] M. H. Osman, M. K. Ahmed, A. Refaat, and N. V. Korovkin, "A comparative study of MPPT for PV system based on modified perturbation & observation method," in *Proc. IEEE Conf. Russian Young Researchers Electr. Electron. Eng. (ElConRus)*, Jan. 2021, pp. 1023–1026.

[41] E. Kim, M. Warner, and I. Bhattacharya, "Adaptive step size incremental conductance based maximum power point tracking (MPPT)," in *Proc. 47th IEEE Photovoltaic Spec. Conf. (PVSC)*, Jun. 2020, pp. 1–5.

[42] A. Aherkar and A. Deshpande, "Fuzzy maximum power point tracking algorithm for photovoltaic system," in *Proc. 2nd IEEE Int. Conf. Recent Trends Electron., Inf. Commun. Technol. (RTEICT)*, May 2017, pp. 1564–1567.

[43] H. S. Agha, Z.-U. Koreshi, and M. B. Khan, "Artificial neural network based maximum power point tracking for solar photovoltaics," in *Proc. Int. Conf. Inf. Commun. Technol. (ICICT)*, Dec. 2017, pp. 150–155.

[44] D. C. Huynh, T. N. Nguyen, M. W. Dunnigan, and M. A. Mueller, "Dynamic particle swarm optimization algorithm based maximum power point tracking of solar photovoltaic panels," in *Proc. IEEE Int. Symp. Ind. Electron.*, May 2013, pp. 1–6.

[45] A. Roy and A. Ghosh, "Current controlled grid-interfaced photovoltaic boost inverter with particle swarm optimisation based MPPT algorithm," in *Proc. Int. Conf. Sustain. Energy Future Electric Transp. (SEFET)*, Jan. 2021, pp. 1–6.

[46] D. C. Huynh, T. M. Nguyen, M. W. Dunnigan, and M. A. Mueller, "Global MPPT of solar PV modules using a dynamic PSO algorithm under partial shading conditions," in *Proc. IEEE Conf. Clean Energy Technol. (CEAT)*, Nov. 2013, pp. 133–138.

[47] H. Li, D. Yang, W. Su, J. Lü, and X. Yu, "An overall distribution particle swarm optimization MPPT algorithm for photovoltaic system under partial shading," *IEEE Trans. Ind. Electron.*, vol. 66, no. 1, pp. 265–275, Jan. 2019.

[48] A. Sharma, A. Sharma, M. Averbukh, V. Jately, and B. Azzopardi, "An effective method for parameter estimation of a solar cell," *Electronics*, vol. 10, no. 312, pp. 1–22, 2021.

[49] H. Ibrahim and N. Anani, "Variations of PV module parameters with irradiance and temperature," *Energy Proc.*, vol. 134, pp. 276–285, Oct. 2017.

[50] D. C. Huynh and M. W. Dunnigan, "Power generation cost minimization of an islanded diesel/wind turbine/fuel cell microgrid system," in *Proc. 5th Int. Conf. Electr., Electron., Commun., Comput. Technol. Optim. Techn. (ICEECCOT)*, Dec. 2021, pp. 1–6.

[51] D. C. Huynh, L. D. Ho, and M. W. Dunnigan, "Optimization of economic environmental and social benefits for integrated energy systems," *J. Eng. Sci. Technol.*, vol. 16, no. 2, pp. 1–17, 2021.

[52] D. C. Huynh and N. Nair, "Chaos PSO algorithm based economic dispatch of hybrid power systems including solar and wind energy sources," in *Proc. IEEE Innov. Smart Grid Technol. Asia (ISGT ASIA)*, Nov. 2015, pp. 1–6.

[53] T. A. Z. Rahman and M. O. Tokhi, "Enhanced stochastic fractal search algorithm with chaos," in *Proc. 7th IEEE Control Syst. Graduate Res. Colloq. (ICSGRC)*, Aug. 2016, pp. 22–27.

[54] O. Bingol, U. Guvenc, S. Duman, and S. Pacaci, "Stochastic fractal search with chaos," in *Proc. Int. Artif. Intell. Data Process. Symp. (IDAP)*, Sep. 2017, pp. 1–6.

[55] H. Mosbah and M. El-Hawary, "Power system static state estimation using modified stochastic fractal search technique," in *Proc. IEEE Can. Conf. Electr. Comput. Eng. (CCECE)*, May 2018, pp. 1–4.

[56] C. Huang, Y. Li, and X. Yao, "A survey of automatic parameter tuning methods for metaheuristics," *IEEE Trans. Evol. Comput.*, vol. 24, no. 2, pp. 201–216, Apr. 2020.

[57] E. S. Skakov and V. N. Malysh, "Parameter meta-optimization of metaheuristics of solving specific NP-hard facility location problem," *J. Phys., Conf.*, vol. 973, pp. 1–12, Dec. 2018.
[58] E. Talbi, *Metaheuristics: From Design to Implementation*. Hoboken, NJ, USA: Wiley, 2009.
[59] W. Dillen, G. Lombaert, and M. Schevenels, "Performance assessment of metaheuristic algorithms for structural optimization taking into account the influence of algorithmic control parameters," *Frontiers Built Environ.*, vol. 7, pp. 1–16, Mar. 2021.
[60] D. C. Huynh and M. W. Dunnigan, "Advanced particle swarm optimization algorithms for parameter estimation of a single-phase induction machine," *Int. J. Model., Identificat. Control*, vol. 15, no. 4, pp. 227–240, 2012.
[61] D. C. Huynh and M. W. Dunnigan, "Parameter estimation of an induction machine using advanced particle swarm optimization algorithms," *IET Electr. Power Appl.*, vol. 4, no. 9, pp. 748–760, Nov. 2010.
[62] D. C. Huynh and M. W. Dunnigan, "Parameter estimation of an induction machine using a chaos particle swarm optimization algorithm," in *Proc. 5th IET Int. Conf. Power Electron., Mach. Drives (PEMD)*, 2010, pp. 1–6.

DUY C. HUYNH (Senior Member, IEEE) received the B.E. degree in electrical engineering from the Ho Chi Minh City University of Technology, Ho Chi Minh City, Vietnam, in 2001, the M.E. degree in electrical engineering from Vietnam National University, Ho Chi Minh City, in 2005, and the Ph.D. degree from Heriot-Watt University, Edinburgh, U.K., in 2010. He is currently an Associate Professor at HUTECH University. His research interests include the areas of energy-efficient control and parameter estimation methods of induction machines, power systems, and renewable sources.

MATTHEW W. DUNNIGAN received the B.Sc. degree (Hons.) in electrical and electronic engineering from Glasgow University, Glasgow, U.K., in 1985, and the M.Sc. and Ph.D. degrees from Heriot-Watt University, Edinburgh, U.K., in 1989 and 1994, respectively. He was employed by Ferranti as a Development Engineer in the design of power supplies and control systems for moving optical assemblies and device temperature stabilization, from 1985 to 1988. In 1989, he became a Lecturer at Heriot-Watt University, where he was concerned with the evaluation and reduction of the dynamic coupling between a robotic manipulator and an underwater vehicle. He is currently an Associate Professor and his research grants and interests include the areas of hybrid position/force control of an underwater manipulator, coupled control of manipulator-vehicle systems, nonlinear position/speed control and parameter estimation methods in vector control of induction machines, frequency domain self-tuning/adaptive filter control methods for random vibration, and shock testing using electrodynamic actuators.

CORINA BARBALATA (Member, IEEE) received the B.E. degree in electrical engineering from Transilvania University, Brasov, Romania, in 2011, the M.S. degree in computer vision and robotics, the joint degree from Heriot-Watt University, Edinburgh, U.K., and the University of Burgundy, Dijon, France, in 2013, and the Ph.D. degree in electrical engineering from Heriot-Watt University, in 2017. She is currently an Assistant Professor at Louisiana State University, Baron Rouge, Louisiana, USA. Her research interests include marine robot systems, autonomous mobile-manipulation, co-operative robotics, multi-body control and planning theory, and underwater perception systems and algorithms.